

# Anomalous $\eta/\eta'$ Decays : The Triangle and Box Anomalies

M. Benayoun<sup>(a)</sup>, P. David<sup>(a)</sup>, L. DelBuono<sup>(a)</sup>  
Ph. Leruste<sup>(a)</sup>, H. B. O’Connell<sup>(b)</sup>

<sup>(a)</sup> LPNHE Paris VI/VII, F-75252 Paris, France

<sup>(b)</sup> Fermilab, PO Box 500 MS 109, Batavia IL 60510, USA.

September 10, 2018

## Abstract

We examine the decay modes  $\eta/\eta' \rightarrow \pi^+\pi^-\gamma$  within the context of the Hidden Local Symmetry (HLS) Model. Using numerical information derived in previous fits to  $VP\gamma$  and  $Ve^+e^-$  decay modes in isolation and the  $\rho$  lineshape determined in a previous fit to the pion form factor, we show that all aspects of these decays can be predicted with fair accuracy. Freeing some parameters does not improve the picture. This is interpreted as a strong evidence in favor of the box anomaly in the  $\eta/\eta'$  decays, which occurs at precisely the level expected. We also construct the set of equations defining the amplitudes for  $\eta/\eta' \rightarrow \pi^+\pi^-\gamma$  and  $\eta/\eta' \rightarrow \gamma\gamma$  at the chiral limit, as predicted from the anomalous HLS Lagrangian appropriately broken. This provides a set of four equations depending on only one parameter, instead of three for the traditional set. This is also shown to match the (two–angle, two–decay–constant)  $\eta - \eta'$  mixing scheme recently proposed and is also fairly well fulfilled by the data. The information returned from fits also matches expectations from previously published fits to the  $VP\gamma$  decay modes in isolation.

# 1 Introduction

Interactions and decays of light mesons fit well within the framework of Chiral Perturbation Theory (ChPT) [1]. Strictly speaking, the ChPT framework applies to the octet members of the pseudoscalar sector ( $\pi, K, \eta_8$ ) which behave as Goldstone bosons whose masses vanish at the chiral limit. Relying on the large  $N_c$  limit of QCD, an extended ChPT framework (EChPT) has been defined [2, 3] including the singlet  $\eta_0$  state which keeps a non-zero mass at the chiral limit, but this vanishes in the large  $N_c$  limit. On the other hand, the decays  $\pi^0/\eta/\eta' \rightarrow \gamma\gamma$ , are understood as proceeding from the so-called triangle anomaly. These are accounted for by means of the Wess–Zumino–Witten (WZW) Lagrangian [4, 5] which is also normally incorporated into the ChPT Lagrangian [2, 3].

Other anomalous processes describing the  $(\pi^0\pi^+\pi^-\gamma)$  vertex and the decay mode ( $\eta \rightarrow \pi^+\pi^-\gamma$ ) have been identified long ago within the context of Current Algebra [6] ; they are presently referred to as box anomalies. Triangle and box anomalies are now derived from the WZW Lagrangian. The box anomaly part of the WZW Lagrangian predicts exactly the values of the amplitudes for the couplings  $(\pi^0\pi^+\pi^-\gamma)$ ,  $(\eta\pi^+\pi^-\gamma)$  and  $(\eta'\pi^+\pi^-\gamma)$  at the chiral limit ; however, the momentum dependence of the corresponding amplitudes is not predicted and should be modelled. When dealing with experimental data, this momentum dependence is naturally accounted for by vector meson contributions and, then, the question becomes whether these alone account for the box anomalies or whether an additional contact term (possibly simulating high mass resonances) is needed ; if this contact term (CT) is needed, it should have a definite value in order to stay consistent with the rigorous predictions of the WZW Lagrangian.

Therefore, from an experimental point of view, the question of the relevance of the box anomaly phenomenon turns out to check the need for a well-defined contact term besides the usual resonant contributions. This question is still awaiting a definite and unambiguous signature.

In its simplest figure, the problem of the relevance of the box anomaly phenomenon is addressed in the coupling  $(\pi^0\pi^+\pi^-\gamma)$ . The relevance of a possible contact term beside vector meson exchanges has been examined. A value for this coupling has been extracted from experimental data [7] and found close to expectations<sup>1</sup> (only  $2\sigma$  apart).

A cleaner environment could be provided by the decay modes  $\eta/\eta' \rightarrow \pi^+\pi^-\gamma$  which are also accounted for in the WZW Lagrangian. Several pieces of information are available : the partial widths [9] are known with an accuracy of the order 10% cross-checked by several means, the  $\eta$  spectrum as function of the photon momentum has been measured long ago [10, 11] and provides useful information. Finally, measurements of the  $\eta'$  spectrum as function of the dipion invariant-mass have been performed twelve times, with various levels of precision, and the corresponding data are published as papers from several Collaborations [13, 14, 15, 16, 17, 18] or are available as PhD theses [19, 20, 21, 22]. The latest measurements have been performed recently by CERN Collaborations [23, 24].

This already represents a large amount of information covering all aspects of these decays. This should allow a reasonably well founded analysis in a search for the box

---

<sup>1</sup>See, also, the discussion in [8].

anomaly in the  $\eta/\eta'$  system.

As stated above, predictions on box anomalies are given at the chiral point and  $\eta/\eta'$  spectra clearly extend in regions where accounting for the  $\rho$  exchange cannot be avoided in order to match experimental information. The magnitude of the  $\eta/\eta' \rightarrow \pi^+\pi^-\gamma$  partial widths should also be influenced by the  $\rho$  exchange. Stated otherwise, including momentum (invariant–mass) dependence within their spectra is essential and should be done in a consistent way in order to extract reliably information on the box anomaly from data.

Indeed, in these decays, two contributions are a priori competing : a contact term and a (dominant) resonant one –the  $\rho$  exchange– with contributions of (sometimes) very different magnitudes. In order to detect reliably the former, the latter has to be known with enough accuracy and, possibly, fixed. The sharing in the anomalous amplitudes at the chiral limit between the contact term and the resonant term might also have to be understood unambiguously.

Therefore, a global framework is needed where the vector meson degrees of freedom are explicitly accounted for together with pseudoscalar mesons and the contact terms. Several such frameworks implementing vector dominance (VMD) in effective Lagrangians have been defined : Resonance Chiral Perturbation Theory [1, 25], massive Yang–Mills fields [26, 27, 28], Hidden Local Symmetry (HLS) Model [29, 30]. It was soon shown [31] that all these approaches were physically equivalent. For convenience, we work within the HLS Model context.

A second issue makes the difference between the  $\pi^0$  box anomaly and the  $\eta/\eta'$  ones. The former is practically insensitive to symmetry breaking effects (Isospin Symmetry breaking is a small effect), the latter however sharply depends on how SU(3) Symmetry and Nonet Symmetry breakings really take place. Therefore a reliable breaking scheme of the  $\eta/\eta'$  sector should also be defined and checked in the triangle and box anomaly sectors. It should also be validated in all processes where it has to apply, like  $V \rightarrow P\gamma$  and  $P \rightarrow V\gamma$  decays. One has already noted some confusion [32] in the meaning of the decay constants entering the amplitudes for the  $\eta$  and  $\eta'$  decays to two photons.

If one limits oneself to collecting some VMD term for the  $\rho$  contribution (even if motivated) and simply adds it with a phase space term to be fit, one can be led to ambiguities [33, 34] when solving the Chanowitz equations [35] which represent the traditional way of describing the  $\eta/\eta'$  mixing (see also [36]). Along the same line, if the breaking scheme generally used [33, 35, 36, 37, 38] happens to be inappropriate in order to describe the  $\eta/\eta'$  system, extracting the box anomaly constant values from data becomes hazardous.

A scheme for implementing SU(3) symmetry breaking in the full HLS Lagrangian has been already defined [39, 40]. This scheme, referred to as BKY has been proved [32] to meet all (E)ChPT requirements and allows a successful account of a very large set of experimental data [41, 42]. A brief global account of the full breaking scheme we advocate is summarized in Appendix A to [43]. The non–anomalous sector has been used in pion

form factor studies providing also consistent results [44, 43].

Therefore, in this paper, we intend to extend the realm of the broken HLS model by studying the decays  $\eta/\eta' \rightarrow \pi^+\pi^-\gamma$ . The behaviour of the model can then be examined in a context where the box anomaly phenomenon is expected to be present. One can hope extracting unambiguously the information about the relevance of this phenomenon from experimental data.

The paper is organized as follows ; in Section 2 we recall the traditional expressions of the decay amplitudes at the chiral limit for  $\eta/\eta' \rightarrow \gamma\gamma$  and  $\eta/\eta' \rightarrow \pi^+\pi^-\gamma$ . In Section 3, we outline the derivation of the full anomalous sector of the HLS Model, mostly referring to the basic paper [30]. In Section 4 we recall shortly how the BKY breaking of SU(3) Symmetry and the breaking of Nonet Symmetry has been performed and tested. In Section 5, we recall the result of applying this to  $\eta/\eta' \rightarrow \gamma\gamma$  as it provides an unconventional set of expressions for the amplitudes at the chiral limit.

In Section 6, we develop the structure predicted for the  $\eta/\eta' \rightarrow \pi^+\pi^-\gamma$  decay modes by the broken HLS Model. We first show that the BKY breaking scheme provides also unconventional expressions for the box anomaly amplitudes at the chiral limit. We also show that all information related with these decay modes (parameters and  $\rho$  meson lineshape) have been already derived numerically and functionally in other sectors of the low energy phenomenology. It thus follows that all properties of the  $\eta/\eta' \rightarrow \pi^+\pi^-\gamma$  decay modes can be predicted without any numerical or functional freedom. In Section 7, we examine the predictions of this model for the  $\eta/\eta' \rightarrow \pi^+\pi^-\gamma$  partial widths and for their dipion invariant-mass spectra.

After reviewing shortly the status of the available experimental data on this subject in Section 8, we devote Section 9 to comparing the predicted lineshapes with the published experimental spectra. Section 10 is devoted to performing a global fit of the shape and yield information for the  $\eta/\eta' \rightarrow \pi^+\pi^-\gamma$  modes in order to check precisely the relevance of the numerical parameters which were all fixed from analysis of other independent data sets. In Section 11, we propose, for comparison, fits of the anomalous amplitudes at the chiral limit, under various conditions and show that the one (instead of three, usually) parameter dependence of these gets a strong support from data.

Finally, Section 12 is devoted to a summary of the results obtained and to conclusions.

## 2 Radiative Decays of Neutral Pseudoscalar Mesons

Some interactions (or decay modes) of neutral pseudoscalar mesons ( $P = \pi^0, \eta, \eta'$ ) are described by matrix elements having the wrong parity and are called anomalous. Anomalous interactions were treated by Wess and Zumino [4] and then expounded upon by Witten [5] ; they are given by the anomalous action, which we shall refer to as  $\Gamma_{\text{WZW}}$ . For the purpose of this paper, two pieces<sup>2</sup> from  $\Gamma_{\text{WZW}}$  are relevant :

---

<sup>2</sup>Here and in the following, we denote by  $V$  the (massive) vector field matrix, by  $A$  the electromagnetic field and by  $P$  the pseudoscalar field matrix. The matrix normalization we use for these have defined

$$\begin{aligned}
\mathcal{L}_{\gamma\gamma P} &= -\frac{N_c e^2}{4\pi^2 f_\pi} \epsilon^{\mu\nu\rho\sigma} \partial_\mu A_\nu \partial_\rho A_\sigma \text{Tr}[Q^2 P] \\
\mathcal{L}_{\gamma PPP} &= -\frac{ieN_c}{3\pi^2 f_\pi^3} \epsilon^{\mu\nu\rho\sigma} A_\mu \text{Tr}[Q \partial_\nu P \partial_\rho P \partial_\sigma P]
\end{aligned} \tag{1}$$

with  $e^2 = 4\pi\alpha$ , and  $f_\pi = 92.42$  MeV ;  $Q$  is the quark charge matrix given by<sup>3</sup>  $A$  is the electromagnetic field and  $P$  is the *bare* pseudoscalar field matrix. From there, amplitude intensities at the chiral point can be derived.

The first piece  $\mathcal{L}_{\gamma\gamma P}$  describes the decays  $\pi^0/\eta/\eta' \rightarrow \gamma\gamma$ . The second piece  $\mathcal{L}_{\gamma PPP}$  contains an interaction term  $\gamma \rightarrow \pi^+\pi^0\pi^-$  briefly discussed in the Introduction. This last piece contains also terms which account for the anomalous decay modes  $\eta/\eta' \rightarrow \pi^+\pi^-\gamma$ .

Without introducing symmetry breaking effects, the Lagrangian pieces in Eq. (1) can give reliable predictions for processes involving only pions. In order to deal with interactions involving  $\eta$  or  $\eta'$  mesons, one has to feed these Lagrangians with SU(3) and Nonet Symmetry breaking mechanisms. Usually these breaking mechanisms are considered to arise from the naive replacement of the pseudoscalar decay constants [35, 36, 8, 37, 48]. Using obvious notations, the amplitudes at the chiral point derived from Eqs. (1) can be written :

$$\begin{aligned}
T(X \rightarrow \gamma\gamma) &= B_X(0) \epsilon^{\mu\nu\rho\sigma} \epsilon_\mu \epsilon'_\nu k_\rho k'_\sigma \\
T(X \rightarrow \pi^+\pi^-\gamma) &= E_X(0) \epsilon^{\mu\nu\rho\sigma} \epsilon_\mu k_\nu p_\rho^+ p_\sigma^-
\end{aligned} \tag{2}$$

( $X = \eta, \eta'$ ), where the coefficients are, assuming  $N_c = 3$  :

$$\begin{aligned}
B_\eta(0) &= -\frac{\alpha}{\pi\sqrt{3}} \left[ \frac{\cos \theta_P}{f_8} - 2\sqrt{2} \frac{\sin \theta_P}{f_0} \right] \\
B_{\eta'}(0) &= -\frac{\alpha}{\pi\sqrt{3}} \left[ \frac{\sin \theta_P}{f_8} + 2\sqrt{2} \frac{\cos \theta_P}{f_0} \right] \\
E_\eta(0) &= -\frac{e}{4\pi^2\sqrt{3}} \frac{1}{f_\pi^2} \left[ \frac{\cos \theta_P}{f_8} - \sqrt{2} \frac{\sin \theta_P}{f_0} \right] \\
E_{\eta'}(0) &= -\frac{e}{4\pi^2\sqrt{3}} \frac{1}{f_\pi^2} \left[ \frac{\sin \theta_P}{f_8} + \sqrt{2} \frac{\cos \theta_P}{f_0} \right]
\end{aligned} \tag{3}$$

using the traditional one-angle mixing scheme. The procedure is thus obvious : one replaces one power of  $f_\pi$  by the octet ( $f_8$ ) or singlet ( $f_0$ ) decay constant understood under their customary definitions in (Extended) ChPT. In the following, we refer to  $X \rightarrow \gamma\gamma$  and  $X \rightarrow \pi^+\pi^-\gamma$  as triangle and box anomalies.

---

in [29, 40, 32] ; our normalization for the SU(3) flavor matrices differs from those in [8] by a factor of 2 :  $T_{Holstein}^a = T_{Witten} = 2 T_{HLS}^a$ . Moreover, we use without distinction  $VP\gamma$  and  $AVP$  to name the corresponding coupling.

<sup>3</sup>There is an intimate connection between the charge of quarks and the value of  $N_c$  in the anomalous action [45, 46, 47] ;  $Q = \text{Diag}(2/3, -1/3, -1/3)$  if  $N_c = 3$ .

This implies several assumptions which are traditionally made in an implicit way [8,37] :

- the decay constant  $f_8$  and  $f_0$  are the (usual) decay constants of ChPT defined from current expectation values :  $\langle 0|J_\mu^8|\eta_8(q)\rangle = if_8q_\mu$  and  $\langle 0|J_\mu^0|\eta_0(q)\rangle = if_0q_\mu$ ,
- SU(3) and Nonet Symmetry Breakings act in exactly the same way for the triangle and box anomalies.

These equations have been used in several ways and they underlie decades of phenomenological work on the  $\eta/\eta'$  mixing. For instance, Refs. [36,8,37] consider the two-photon decay widths of the  $\eta$  and  $\eta'$  mesons and the ratio  $f_8/f_\pi \simeq 1.3$  from ChPT [1] to derive  $\theta_P \simeq -20^\circ$  and  $f_0/f_\pi \simeq 1.04$  ; this meets ChPT expectations [2,3] if one identifies  $\theta_P$  with the presently named  $\theta_8$ . Comparable results [34,38] are derived by using the four equations above, after extracting the box anomaly constants from the dipion mass spectra in  $\eta/\eta' \rightarrow \pi^+\pi^-\gamma$  decays. The third Eq. (3) has also been used with accepted parameter values ( $f_8/f_\pi = 1.25$ ,  $f_0/f_\pi = 1.04$  and  $\theta_P = -20.6^\circ$ ) inside the HLS Model to derive a successful description of  $\eta \rightarrow \pi^+\pi^-\gamma$  in isolation [49].

The validity of the first two Eqs. (3) has been recently addressed and consistency of these with the  $\eta/\eta'$  breaking scheme derived from EChPT [2,3] has been found doubtful [32,50,51].

There is no currently known examination of the last two Eqs. (3) ; however, some remarks on the renormalization of the WZW box term [40] tend to indicate that these are also doubtful. Therefore, the phenomenological results derived from using Eqs. (3) have to be reexamined in a consistent framework.

### 3 The Anomalous Sector in the HLS Model

The HLS Model originally describes the  $\gamma - V$  transitions, all couplings of the kind  $VPP$  and possibly  $APP$ , if the specific parameter  $a$  of the HLS model [29] is not fixed in order to recover the traditional VMD formulation ( $a = 2$ ). In this framework, the main decay mode  $\omega \rightarrow \pi^+\pi^0\pi^-$  of the  $\omega$  meson is, for instance, absent as clear from the explicit expression of the HLS Lagrangian [40].

As seen above, anomalous interactions involving pseudoscalar mesons and photons are contained in  $\Gamma_{WZW}$  [4,5]. These terms were included in the Hidden Local Symmetry Lagrangian by Fujiwara *et al.* [30], along with anomalous vector meson ( $V$ ) interactions in such a way that the low energy anomalous processes (in the chiral limit where  $m_\pi = 0$ )  $\gamma \rightarrow \pi^+\pi^0\pi^-$  and  $\pi^0 \rightarrow \gamma\gamma$  are solely predicted by  $\Gamma_{WZW}$ . The construction of this HLS anomalous Lagrangian, originally performed in [30], is discussed in detail in several excellent reviews [28,39]. Here, we limit ourselves to a brief outline of its derivation, pointing out the motivation for some important assumptions. The anomalous action has

the form :

$$\begin{aligned}\Gamma &= \Gamma_{\text{WZW}} + \Gamma_{\text{FKTUY}} \\ \Gamma_{\text{FKTUY}} &= \sum_{i=1}^4 c_i \int d^4x \mathcal{L}_i\end{aligned}\tag{4}$$

where the  $c_i$  are entirely arbitrary constants. The Lagrangians  $\mathcal{L}_i$  are given in [30] and each of them contains *APPP* and *AAP* pieces which would contribute to the anomalous decays, but are cancelled by *APV* terms. These Lagrangians contain also *VPPP* and *VVP* pieces [30].

In view of extending the assumption of dominance of vector mesons (VMD) to the anomalous sector, it was first shown that a set of  $c_i$  in Eq. (4) can be defined in such a way that  $\pi^0 \rightarrow \gamma\gamma$  occurs solely through  $\pi^0 \rightarrow \omega\rho^0$  followed by the (non-anomalous) transitions  $\omega \rightarrow \gamma$  and  $\rho^0 \rightarrow \gamma$ . The  $\pi^0$  width thus derived is identical to the Current Algebra prediction reproduced by  $\mathcal{L}_{\gamma\gamma P}$  defined in the previous Section.

It was also shown [30] that complete vector dominance can be achieved, where the direct term *APPP* is converted to *VPPP*, with some other set of  $c_i$ . In this framework, the decay  $\omega \rightarrow \pi^+\pi^0\pi^-$  occurs through  $\omega \rightarrow \pi^0\rho^0$  (the *VVP* term) followed by  $\rho^0 \rightarrow \pi^+\pi^-$  and through the contact term (*VPPP*) which gives a direct contribution  $\omega \rightarrow \pi^+\pi^0\pi^-$ . However, it happens that the *VVP* contribution (which provides alone the correct  $\omega$  partial width) is numerically reduced in a significant way by the contact term (*VPPP*). In view of this, [30] proposes another set of  $c_i$  which provides an anomalous effective Lagrangian containing only a *VVP* term and, besides, the standard WZW term *APPP* in the following combination :

$$\mathcal{L}^{\text{FKTUY}} = -\frac{3g^2}{4\pi^2}\epsilon^{\mu\nu\rho\sigma}\text{Tr}[\partial_\mu V_\nu\partial_\rho V_\sigma P] - \frac{1}{2}\mathcal{L}_{\gamma PPP} \ ,\tag{5}$$

where  $\mathcal{L}_{\gamma PPP}$  is defined in Eqs. (1). One should note that the normalization affecting the WZW part of this Lagrangian is a pure prediction of the HLS Model based on a definite extension of the VMD concept to anomalous processes.

Focussing on decays like  $\eta/\eta' \rightarrow \pi^+\pi^-\gamma$ , one readily sees from this expression that, in order to recover the behaviour expected from  $\mathcal{L}_{\gamma PPP}$  alone, these two terms should contribute to the box anomaly (*i.e.* the full amplitude at the chiral limit) in the following ratio :

$$\text{VMD} : \text{CT} = -3 : 1 \ ,$$

at the chiral limit ; “VMD” names here the contribution generated by the first term in Eq. (5) and “CT” (contact term) those generated from the second term. Thus, the “VMD” contribution, generated by the triangle anomaly generalized to *VVP* couplings, is predicted dominant at the chiral limit.

Within this framework, the main  $\omega$  decay mode proceeds only from  $\omega \rightarrow \rho^0\pi^0$  followed by  $\rho^0 \rightarrow \pi^+\pi^-$  and  $\phi \rightarrow \pi^+\pi^-\pi^0$  proceeds solely from  $\omega - \phi$  mixing. The experimental situation concerning the decay mode  $\phi \rightarrow \pi^+\pi^-\pi^0$  is conflicting. Indeed, a recent result from the SND Collaboration [52] claims for no significant evidence in favor of a contact

$\phi \rightarrow \pi^+\pi^-\pi^0$  term in their  $e^+e^- \rightarrow \pi^+\pi^-\pi^0$  data and provides a new upper bound much more stringent than previous ones [9] ; however, using their own data on the same physical process, the KLOE Collaboration [53] claims that a significant contact term is present in their data. Actually, as there is currently no available analysis performed using consistently a full VVP and VPPP Lagrangian or a Lagrangian like in Eq. (5), no founded conclusion can really be drawn.

Processes like  $\pi^0/\eta/\eta' \rightarrow \gamma\gamma$  occur solely through  $\pi^0/\eta/\eta' \rightarrow VV'$  followed by  $V, V' \rightarrow \gamma$ . However, transitions like  $\gamma \rightarrow \pi^+\pi^0\pi^-$  or decays like  $\eta/\eta' \rightarrow \pi^+\pi^-\gamma$  receive contributions from the contact term and from the VVP term (essentially through  $\rho$  meson exchange).

The VVP piece of this effective Lagrangian has been used successfully in several recent studies [41, 42, 32, 55] and proved to predict (after implementing appropriate symmetry breaking mechanisms) up to 26 physics information with a number of free independent parameters ranging from 6 to 9 (when Isospin Symmetry breaking is considered [55]).

## 4 The Extended BKY Symmetry Breaking Scheme

The study of SU(3) breaking of the HLS Model has been initiated by BKY [39] who proposed a simple and elegant mechanism. However, the procedure was soon understood as breaking also Hermiticity of the derived Lagrangian, which was clearly an undesired feature. A slight modification [40] of the original BKY procedure was shown to cure this problem and to produce a quite acceptable broken Lagrangian (see Eq. (A5) in [40]). The way field renormalization has to be performed turns out to define the renormalized field matrix (denoted  $P'$ ) in terms of the bare field matrix (denoted  $P$ ) by :

$$P = X_A^{-1/2} P' X_A^{-1/2} \quad , \quad (6)$$

where the breaking matrix is  $X_A = \text{Diag}(1, 1, z)$ , with  $z = [f_K/f_\pi]^2$ .

As such, the (original) BKY breaking scheme can only address a limited amount of physics processes, as all information related with the  $\eta$  meson can only be treated crudely and the properties of the  $\eta'$  meson cannot be addressed.

In order to address physics information about the  $\eta/\eta'$  system appropriately, the singlet sector has first to be introduced in the original HLS Lagrangian. This has been done by using [40] the U(3) symmetric field matrix  $P = P_8 + P_0$  instead of only  $P = P_8$  when constructing the Lagrangian. This is found to provide the HLS Lagrangian with the canonical kinetic energy of the singlet state ( $\eta_0$  field) while this does not modify the interaction Lagrangian [40] by adding  $\eta_0$ -dependent pieces.

The step further is to break the  $U_A(1)$  symmetry by introducing determinant terms [56] into the effective Lagrangian which becomes [32] :

$$\mathcal{L} = \mathcal{L}_{HLS} - \frac{1}{2}\mu^2\eta_0^2 + \frac{1}{2}\lambda\partial_\mu\eta_0\partial^\mu\eta_0 \quad (7)$$



By means of this (modified) BKY breaking scheme, the HLS Lagrangian can now address the  $\eta/\eta'$  system with a complete scheme of symmetry breaking (SU(3) and Nonet Symmetries). A  $\eta_0$  mass term is generated and the kinetic energy term of the Lagrangian is modified in a non-canonical way, which implies that a field transformation to renormalized fields has to be performed. This can be done through the two-step renormalization procedure defined in [32] and outlined in the Appendix. This transformation is well approximated [32] by :

$$P = X_A^{-1/2} [P'_8 + xP'_0] X_A^{-1/2} \quad ; \quad (8)$$

this has been shown to differ [32] from the exact field transformation only by terms of second order in the breaking parameters ( $[z - 1]$ ,  $[x - 1]$ ).

This transformation <sup>4</sup> was postulated (or fortunately anticipated) in [41] in order to study the full set of  $AVP$  radiative decays, especially the modes involving the  $\eta/\eta'$  mesons. Using this transformation has provided a fairly good description of the whole physics accessible to this broken Lagrangian [41, 32, 42, 55] with only a small number of parameters, as already noted.

Departures from Nonet Symmetry were observed [41] by extracting from data  $x = 0.90 \pm 0.02$ , significantly different from 1. One may rise the question of the correspondance between  $x$  in Eq. (8) and the basic Nonet Symmetry breaking parameter  $\lambda$  of the Lagrangian in Eq. (7) – which is [32] nothing but the  $\Lambda_1$  parameter of [2, 3]. One can write :

$$x = \frac{1}{\sqrt{1 + h\lambda}} \quad , \quad h = 1 + \mathcal{O}(z - 1) \quad . \quad (9)$$

Indeed, as shown in the Appendix,  $x$  absorbs a small influence of SU(3) symmetry breaking (about 5% of its fitted value).

Comparison of all results of this broken HLS Lagrangian, especially decay constants and mixing angles, with the available (E)ChPT estimates of the same parameters [2, 3, 50] was done and appeared also fully satisfactory. It is worth remarking that the HLS phenomenology was yielding an estimate for the (E)ChPT mixing angle  $\theta_0$  much smaller in magnitude than the (E)ChPT leading order estimate ( $-0.05^\circ \pm 0.99^\circ$  in contrast with  $\simeq -4^\circ$ ), but in fair correspondance with a more recent EChPT next-to-leading order calculation [58] which yields  $\theta_0 = [-2.5^\circ, +0.5^\circ]$ .

It is also worth remarking that the (full) breaking scheme just outlined anticipated [41] the branching fraction for  $\phi \rightarrow \eta'\gamma$  with a value twice smaller than its contemporary measurement [54]. This predicted value coincides with all recent measurements performed with larger statistics [9].

The quasi-vanishing of  $\theta_0$  has two interesting consequences. On the one hand, it allows to relate the traditional wave-function mixing angle with the recently defined  $\theta_8$

---

<sup>4</sup>The motivation behind this postulate was that weighting differently the singlet and octet parts of the  $P$  and  $V$  field matrices allows to derive the most general parametrization [57] of the  $VP\gamma$  coupling constants consistent with only SU(3) symmetry in the vector and pseudoscalar sectors, while the corresponding U(3) symmetries are both broken.

mixing angle [2,3] by providing  $\theta_8 \simeq 2\theta_P$  (fulfilled at a few percent level) ; the derivation is given in the Appendix for the exact field transformation.

On the other hand, the condition  $\theta_0 = 0$  relates the Nonet symmetry breaking parameter  $x$  to  $\theta_P$  :

$$\tan \theta_P = \sqrt{2} \frac{(1-z)}{2+z} x \quad (10)$$

This relation is fulfilled with a high degree of numerical accuracy [32] and only reflects that the ChPT mixing angle  $\theta_0$  is not significantly affected by symmetry breaking effects. This relation will be somewhat refined (See Section 11 and the Appendix).

It then follows that, from the three originally free breaking parameters associated with the pseudoscalar sector ( $z, x, \theta_P$ ), only one remains unconstrained. It could be either of  $x$  or  $\theta_P$  ; however, it will be shown that  $x$  might be preferred.

We do not go on discussing here symmetry breaking in the vector meson sector as it is not in the stream of the present paper ; we refer interested readers to [39,40,41,42] where this is discussed in details.

Some remarks are of relevance. The combined Nonet Symmetry and SU(3) breaking scheme of the HLS Lagrangian presented in this Section defines what we name the Extended BKY breaking scheme. It restores the relevance of a one angle mixing scheme for the  $\eta/\eta'$  system. However, this does not give any support to the traditional breaking scheme as expressed by Eqs. (3). In contrast, it matches fairly well all expectations of the two-angle, two-coupling constant mixing scheme recently derived from EChPT [2,3,50,51] at leading order in the breaking parameters.

This full breaking scheme is also mathematically equivalent to the recently proposed [50,51] breaking in the quark flavor basis framework ; it might be preferred as a definite concept like Nonet Symmetry breaking, which underlies some Lagrangian pieces ( $\mathcal{L}_2$ ) of EChPT, can be implemented more clearly and tracing its effect in phenomenology is easier.

## 5 Two-Photon Decay Widths of the $\eta$ and $\eta'$ mesons

The two-photon decay widths of the  $\eta$  and  $\eta'$  mesons can be derived easily from the HLS Lagrangian (the  $VVP$  part of Eq. (5)) supplemented by the  $V\gamma$  transition amplitudes of the non-anomalous HLS Lagrangian) after renormalizing to physical fields by Eq. (8). Applying directly the same Eq. (8) to the WZW Lagrangian  $\mathcal{L}_{\gamma\gamma P}$  in Eq. (1) leads exactly to the same result<sup>5</sup> [32] :

$$\begin{aligned} G_\eta(0) &= -\frac{\alpha}{\pi\sqrt{3}f_\pi} \left[ \frac{5z-2}{3z} \cos \theta_P - \sqrt{2} \frac{5z+1}{3z} x \sin \theta_P \right], \\ G_{\eta'}(0) &= -\frac{\alpha}{\pi\sqrt{3}f_\pi} \left[ \frac{5z-2}{3z} \sin \theta_P + \sqrt{2} \frac{5z+1}{3z} x \cos \theta_P \right]. \end{aligned} \quad (11)$$

---

<sup>5</sup>From now on, we assume  $N_c = 3$ .

These expressions compare well with the corresponding quantities in Eqs. (3). However, this correspondence is only formal as, defining  $\bar{f}_8$  and  $\bar{f}_0$  by :

$$\frac{f_\pi}{\bar{f}_8} = \frac{5z - 2}{3z}, \quad \frac{f_\pi}{\bar{f}_0} = \frac{5z + 1}{6z} x, \quad (12)$$

yields  $\bar{f}_8 = 0.82f_\pi$  (and  $\bar{f}_0 = 1.17f_\pi$ ), which has little to do with numerical expectations from ChPT (extended or not). It was proved in [32] that these are *not* the standard EChPT decay constants. These can be derived from our broken Lagrangian, yielding information which matches [32] fairly well EChPT expectations [2,3].

This proved the basic consistency of breaking scheme presented in the previous Section with EChPT. The formulation given in Eq. (11) could look, at leading order, more tractable than present standard expressions ; it makes indeed much clearer that the number of parameters to be determined phenomenologically is limited.

Therefore, the first basic assumption which underlies the understanding of Eqs. (3) is not fulfilled by the BKY breaking scheme [39,40] and this is independent of whether Nonet Symmetry is broken.

Let us remind that Eqs. (11) give the two-photon radiative decay widths of the  $\eta/\eta'$  mesons with good accuracy. These can even be predicted by using solely the value of  $x$  extracted from fit to the (independent) set of  $AVP$  decay modes of light mesons [32]. Fixing  $z = [f_K/f_\pi]^2$  to its experimental value and assuming Eq. (10), Eqs. (11) become a constrained system depending on only one parameter and can be solved providing results consistent with using, instead, the  $AVP$  decay mode information.

Of course, the mixing angle  $\theta_P$  entering Eqs. (11) does not coincide with  $\theta_8$  and is derived [32] as  $\theta_P = -10.32^\circ \pm 0.20^\circ$  when requiring the constraint Eq. (10) to hold exactly ; the corresponding value for  $\theta_8 \simeq -20^\circ$  compares well to expectations [1,2,3]. One should note a recent estimate of  $\theta_P = -10^\circ \pm 2^\circ$  provided by lattice QCD computations [59] which strongly supports this phenomenologically extracted value.

Therefore, the picture represented by Eqs. (11), which does not meet traditional expectations [8, 38, 58, 34], matches quite well all relevant information from ChPT and QCD, and, last but not least, corresponds to a satisfactory description of the whole set of two-body radiative decays of light mesons [41, 42, 32].

## 6 The HLS Model For $\eta/\eta' \rightarrow \pi^+\pi^-\gamma$ Decay Modes

Using the effective Lagrangian in Eq. (5), the processes  $\eta/\eta' \rightarrow \pi^+\pi^-\gamma$  receive VMD contributions from the  $VVP$  term and CT contributions from the  $\mathcal{L}_{\gamma PPP}$  piece. The purpose of this Section is to examine carefully these decay modes. These will also lead us to question the last two (box) anomaly equations Eqs. (3).

## 6.1 Basic Lagrangians

Within the HLS Model, the  $VVP$  part of  $\eta/\eta' \rightarrow \pi^+\pi^-\gamma$  involves, beside the  $\rho$  meson, the interplay of the  $\omega$  and  $\phi$  mesons to their decay mode to  $\pi\pi$  only<sup>6</sup>. However, these (isospin violating) couplings are small enough to be safely neglected. Additionally, the  $\phi$  meson is outside the decay phase space of both  $\eta$  and  $\eta'$  mesons, and the accuracy of the data is far from allowing any  $\omega$  effect to be significant or simply visible in the  $\eta'$  dipion invariant-mass spectrum.

It can be shown [42], that the  $VP\gamma$  couplings following from the anomalous sector of HLS model can be derived from the corresponding ( $VP\gamma$ ) piece of :

$$\mathcal{L} = C\epsilon^{\mu\nu\rho\sigma}\text{Tr}[\partial_\mu(eQA_\nu + gV_\nu)\partial_\rho(eQA_\sigma + gV_\sigma)X_A^{-1/2}(P'_8 + xP'_0)X_A^{-1/2}] \quad , \quad (13)$$

where  $g$  is the universal vector coupling of the HLS Model [29]. The value for  $C = -3/(4\pi^2 f_\pi)$  is fixed by normalizing the  $AAP$  term in Eq. (13) to the corresponding WZW Lagrangian in Eq. (1).

This equation could essentially be considered as a way to postulate VMD for  $VVP$  couplings and it also gives the normalization shown in Eq. (5). Focussing on the piece of Eq. (13) related with neutral pseudoscalar mesons, one gets :

$$\mathcal{L}_{\gamma\rho P^0} = -\frac{eg}{4\pi^2 f_\pi} \left[ \frac{1}{2}\pi^0 + \frac{\sqrt{3}}{2}\eta_8 + x\sqrt{\frac{3}{2}}\eta_0 \right] \epsilon^{\mu\nu\alpha\beta} \partial_\mu A_\nu \partial_\alpha \rho_\beta^0 \quad , \quad (14)$$

with obvious notations. The  $\rho$  meson decay relevant for the present study is driven by :

$$\mathcal{L}_{\rho\pi\pi} = i\frac{ag}{2}\rho_\mu^0 [\pi^-\partial^\mu\pi^+ - \pi^+\partial^\mu\pi^-] \quad (15)$$

which can be extracted from the non-anomalous (broken or not) HLS Lagrangian. The parameter  $a$  is the specific HLS parameter expected such that  $a = 2$  in traditional formulations of VMD, but has always been fitted in the range  $a = 2.3 \div 2.5$  from radiative and leptonic decays of light mesons [41, 42] and in pion form factor studies [44, 60]. We recall that the  $\rho$  mass in the HLS Model is not free and is given by the (extended) KSFR relation  $m_\rho^2 = ag^2 f_\pi^2$  which does not coincide with traditional mass values [9] ( $\simeq 830$  MeV versus  $\simeq 775$  MeV) ; these happen to be only a matter of definition [43]. Finally, the CT contributions are contained in the following Lagrangian piece extracted from Eq. (5) –for the normalization– and Eq. (1) :

$$\mathcal{L}_{\gamma\pi^+\pi^-P^0} = -i\frac{e}{8\pi^2 f_\pi^3} \epsilon^{\mu\nu\alpha\beta} A_\mu \partial_\nu \pi^+ \partial_\alpha \pi^- \left[ \partial_\beta \pi^0 + \frac{1}{\sqrt{3}}\partial_\beta \eta_8 + x\sqrt{\frac{2}{3}}\partial_\beta \eta_0 \right] \quad . \quad (16)$$

---

<sup>6</sup>Indeed, the non-anomalous HLS Lagrangian, broken or not [40], contains no couplings like  $\eta\pi V$  or  $\eta'\pi V$ . Therefore, terms like  $\eta/\eta' \rightarrow \pi V$  followed by  $V \rightarrow \pi\gamma$  do not contribute to the decays under examination.

Changing from  $\eta_8, \eta_0$  to  $\eta, \eta'$  is performed by a rotation involving the (wave-function) mixing angle :

$$\begin{bmatrix} \eta \\ \eta' \end{bmatrix} = \begin{bmatrix} \cos \theta_P & -\sin \theta_P \\ \sin \theta_P & \cos \theta_P \end{bmatrix} \begin{bmatrix} \eta_8 \\ \eta_0 \end{bmatrix} \quad (17)$$

There is, obviously, no loss of generality in introducing this definition and, thus, the physical parameter  $\theta_P$  which has to be fixed or fitted.

For all expressions in this Section, the fields which occur are the renormalized ones. It should already be noted that all basic Lagrangian pieces involved in the considered  $\eta/\eta'$  decays do not depend at leading order on the SU(3) breaking mechanism (the parameter  $z = [f_K/f_\pi]^2$  already met), at least in the limit of Isospin Symmetry where we stand. However SU(3) symmetry breaking is hidden inside  $\theta_P$  (see Eq.(10)).

## 6.2 Amplitudes and Chiral Limit Properties

With the information given just above, it is an easy task to compute the amplitudes for the  $\eta/\eta'$  decays considered. One finds :

$$T(X \rightarrow \pi^+ \pi^- \gamma) = c_X \frac{ie}{8\sqrt{3}\pi^2 f_\pi^3} \left[ 1 + \frac{3m_\rho^2}{D_\rho(s)} \right] \epsilon^{\mu\nu\alpha\beta} \epsilon_\mu k_\nu p_\alpha^+ p_\beta^- \quad , \quad (18)$$

using obvious notations, with  $X = \eta, \eta'$ ,  $m_\rho^2 = ag^2 f_\pi^2$  and  $s$  being the dipion invariant-mass. The  $c_X$  are given by :

$$\begin{aligned} c_\eta &= [\cos \theta_P - x\sqrt{2} \sin \theta_P] \quad , \\ c_{\eta'} &= [\sin \theta_P + x\sqrt{2} \cos \theta_P] \quad . \end{aligned} \quad (19)$$

Finally  $D_\rho(s)$  is the inverse  $\rho$  propagator which can be written [43] :

$$D_\rho(s) = s - m_\rho^2 - \Pi_{\rho\rho}(s) \quad , \quad (20)$$

in terms of the already defined (KSFR)  $\rho$  mass and of the  $\rho$  self-mass. The occurrence of  $\Pi_{\rho\rho}(s)$  permits to move the  $\rho$  pole off from the physical region [61, 43]. For the present purpose, one has only to stress that the  $\rho$  self-mass can be chosen rigorously such that  $\Pi_{\rho\rho}(0) = 0$  as expected from current conservation [63].

Going to the chiral limit, Eq. (18) is nothing but the second Eq. (2) and has for coefficients :

$$\begin{aligned} E'_\eta(0) &= -\frac{ie}{4\sqrt{3}\pi^2 f_\pi^3} [\cos \theta_P - x\sqrt{2} \sin \theta_P] \\ E'_{\eta'}(0) &= -\frac{ie}{4\sqrt{3}\pi^2 f_\pi^3} [\sin \theta_P + x\sqrt{2} \cos \theta_P] \quad . \end{aligned} \quad (21)$$

These relations clearly meet expectations of Current Algebra ; they could not be derived exactly if  $\Pi_{\rho\rho}(0) \neq 0$ . The single symmetry breaking parameter occuring manifestly is  $x$  which essentially measures departures from Nonet Symmetry.

It should be noted that there is no obvious connection between the way symmetry breaking occurs for the box anomaly (Eq. (21)) and for the triangle anomaly (see Eqs. (11)) within the broken HLS Model. It is worth recalling once more, that the symmetry breaking scheme defined in Section 4 was shown [32] to match perfectly all expectations of EChPT collected in [2, 3, 50] and that no further piece has been added in order to derive Eqs. (21).

Therefore, the second assumption which underlies the traditional way of breaking symmetries for this set of equations (see the discussion after Eqs. (3)) is also not met by the BKY breaking scheme [39, 40, 32].

Eqs. (21) are also interesting for other aspects : In order to recover the values expected for both  $E'_X(0)$ , the VMD (*i.e.* resonant) contribution happens to be 3 times larger than the contact term (CT) contribution and carries an opposite sign ; this was expected when building the anomalous HLS Lagrangian Eq. (5).

Eqs. (18) also show that fitting the  $\eta/\eta'$  invariant–mass spectra with a constant term interfering with a resonant term is indeed legitimate. However, it is also clear that the value of this constant is *not* the value of the full amplitude at origin and thus carries only a part of the box anomaly value.

The triangle and box anomaly expressions in the broken HLS model are summarized by Eqs. (11) and (21). We know from previous works [41, 32] that experimental data support this in the triangle anomaly sector ( $AVP$  and  $\eta/\eta' \rightarrow \gamma\gamma$ ) ; the real issue is to test its validity in processes where box anomalies are expected to occur.

### 6.3 The $\gamma\pi^+\pi^-\pi^0$ Amplitude

Even if outside the main stream of this paper, it is interesting to give the amplitude for the  $\gamma\pi^+\pi^-\pi^0$  anomalous coupling. Using Eqs. (1) and (14) above, together with the piece analogous to Eq. (15) for  $\rho^\pm$  which can be found in [40], one gets :

$$T(\gamma \rightarrow \pi^+\pi^-\pi^0) = A(s, t, u) \epsilon^{\mu\nu\alpha\beta} \epsilon_\mu p_\nu^+ p_\alpha^- p_\beta^0 \quad , \quad (22)$$

with :

$$A(s, t, u) = \frac{e}{8\pi^2 f_\pi^3} \left[ 1 + \frac{m_\rho^2}{D_\rho(s)} + \frac{m_\rho^2}{D_\rho(t)} + \frac{m_\rho^2}{D_\rho(u)} \right] \quad , \quad (23)$$

where  $m_\rho^2 = ag^2 f_\pi^2$  and  $D_\rho$  is given by Eq. (20) with the appropriate permutation of the argument  $s$  to  $t$  and  $u$ . In this case, the symmetry breaking mechanism we have defined has no influence. The momentum dependence of this expression differs from known ones (recalled by Eqs. (39) and (40) in [8]) by its taking into account the  $\rho$  self–energy (see Eq. (20)). It gives the expected value ( $-ie/4\pi^2 f_\pi^3$ ) at  $s = t = u = 0$  and is worth to be checked on forthcoming experimental data [64]. It might also be extracted from  $e^+e^- \rightarrow \pi^+\pi^-\pi^0$  annihilation with data covering the low invariant–mass region.

## 6.4 Invariant–Mass Spectra And The Box Anomaly

From the amplitude in Eq (18), one derives the decay width :

$$\frac{d\Gamma(X \rightarrow \pi^+\pi^-\gamma)}{d\sqrt{s}} = \frac{c_X^2}{36} \frac{\alpha}{[2\pi f_\pi]^6} \left| 1 + \frac{3m_\rho^2}{D_\rho(s)} \right|^2 k_\gamma^3 q_\pi^3, \quad (24)$$

for each of the  $\eta$  and  $\eta'$  mesons. We have defined  $k_\gamma = (m_X^2 - s)/2m_X$ , the photon momentum in the  $X$  rest frame and  $q_\pi = \sqrt{s - 4m_\pi^2}/2$ , the pion momentum in the dipion rest frame.

The contact term generated by the second piece in Eq. (5), is represented in Eq. (24) by the number 1 inside the modulus squared. On the other hand, as the normalization of the VMD contribution can be fixed [41, 42] at the appropriate value by only normalizing to the  $P\gamma\gamma$  amplitude in Eq. (13), checking the effect of this contact term by switching on/off this “1” in Eq. (24) is indeed meaningful. In this way, one can address the experimental relevance of Eq. (5).

Eq. (24) is interesting in many regards :

- The shape of the invariant–mass spectra depends on the  $\eta/\eta'$  meson properties only through a kinematical factor ( $k_\gamma^3$ ). Therefore, the shape of the invariant–mass spectra does not carry any *manifest* information on the box anomaly constants  $c_X$ ,
- The lineshape of the invariant–mass spectra in  $\eta/\eta'$  decays depends only on  $\rho$  meson properties. However, the way this dependence occurs in  $\eta/\eta'$  decays is different from the one in the pion form factor [43], as the dressing of the  $\rho-\gamma$  transition amplitude  $\Pi_{\rho\gamma}(s)$  plays no role in the  $\eta/\eta'$  decays,
- All information on the value of  $c_\eta$  and  $c_{\eta'}$  is carried by the partial width itself. It can be algebraically derived if  $D_\rho(s)$  is known reliably from another source.

In order to perform a search for the box anomaly, one needs a function  $D_\rho(s)$  accurately determined between the two–pion threshold and the  $\phi$  mass. In the physical region involved in  $\eta/\eta'$  decays, all coupled channels allowed by the HLS model contribute at one–loop order [43]. However, except for  $\pi^+\pi^-$ , each provides<sup>7</sup> only logarithms, beside their influence on the subtraction polynomial hidden inside the  $\rho^0$  self–mass  $\Pi_{\rho\rho}(s)$ . This is their major effect, and thus neglecting these loops while still considering a subtraction polynomial of the appropriate degree is certainly motivated.

Reduced to only its coupling to  $\pi^+\pi^-$  (with or without accounting for kaon pairs), the  $\rho$  propagator used here contributes to providing a fairly accurate numerical determination of the pion form factor both in modulus [43, 61] and in phase [43] up to the  $\phi$  mass.

---

<sup>7</sup>And, to some extent, except also for the  $\omega\pi^0$  channel in the  $\eta'$  decay ; however, the neglected effect is concentrated in the region above 917 MeV, very close to the phase space boundary for  $\eta'$  decay and far beyond in the  $\eta$  decay.

Therefore, for the purpose of studying the box anomaly, there is no point in going beyond contributions from only the non-anomalous HLS Lagrangian. In this case, the  $\rho$  self-energy can be written :

$$\Pi_{\rho\rho}(s) = g_{\rho\pi\pi}^2 [\ell_\pi(s) + \frac{1}{2z^2} \ell_K(s)] \quad , \quad (25)$$

where  $g_{\rho\pi\pi} = ag/2$ , while  $z$  has been already defined. We have denoted  $\ell_\pi(s)$  and  $\ell_K(s)$  the pion and kaon loops amputated from their couplings to external legs (we neglect the mass difference between  $K^\pm$  and  $K^0$ ) ; these are given in closed form in [42].

These loops should be subtracted at least twice in order to make convergent the Dispersion Integrals which define them as analytic functions ; this gives rise to a first degree polynomial  $P_\rho(s)$  with arbitrary coefficients to be determined by imposing explicit conditions or by fit. However, as noted just above, anomalous loops force to perform, at least, three subtractions [42,43], which modifies the arbitrary polynomial  $P_\rho(s)$  to (at least) second degree. It is the reason why  $P_\rho(s)$  will be assumed of second degree, even if one limits oneself to pion and kaon loops. This does not increase our parameter freedom, as will be seen shortly.

## 6.5 External Numerical Information

From what seen above, the condition  $P_\rho(0) = 0$  on the subtraction polynomial is certainly desirable, otherwise the Current Algebra expectations could not be derived exactly ; additionally, this condition ensures masslessness of the photon after dressing by pion and kaon loops. It thus remains 2 subtraction constants to be determined or chosen ; we shall fix them from the fit performed [43] on the pion form factor from threshold to the  $\phi$  mass. Denoting  $\bar{\Pi}_{\rho\rho}(s)$  the  $\rho$  self-energy subtracted three times [42], we have :

$$\Pi_{\rho\rho}(s) = \bar{\Pi}_{\rho\rho}(s) + e_1 s + e_2 s^2 \quad . \quad (26)$$

On the other hand, we can also fix the HLS parameters  $a$ ,  $g$  (and thus  $m_\rho$ ) and  $x$  to their values fitted in radiative and leptonic decays<sup>8</sup> [41,42]. Knowing  $z$  and  $x$ , one can derive the value for  $\theta_P$  from Eq. (10). The values for  $e_1$  and  $e_2$  are fixed from an appropriate fit to the pion form factor [43], where the parameters  $a$ ,  $g$  and  $x$  are fixed consistently with  $AVP$  and  $(\omega/\phi)e^+e^-$  modes.

As we restrict the  $\rho$  coupling to only the  $\pi^+\pi^-$  and  $K\bar{K}$  channels, these values for  $e_1$  and  $e_2$  are certainly correlated with the chosen values for  $a$  and  $g$  ; they are not affected numerically by the value for  $x$ .

The values for these parameters are gathered in Table 1. As these parameters are supposed universal in the realm of the HLS Model, one can fix their values from fit to

---

<sup>8</sup>Actually, the values for  $g$  and  $x$  are determined almost solely by the  $AVP$  radiative decays ; the value for  $a$  is a consequence of these on the  $V \rightarrow e^+e^-$  decay modes, but mostly the  $\omega$  and  $\phi$  leptonic decays.



Parameter	Value
$a$	$2.51 \pm 0.03$
$g$	$5.65 \pm 0.02$
$x$	$0.90 \pm 0.02$
$z = [f_K/f_\pi]^2$	$1.51 \pm 0.02$
$e_1$	$0.222 \pm 0.011$
$e_2$	$-1.203 \pm 0.017 \text{ GeV}^{-2}$

Table 1: Parameter values for  $a$ ,  $g$ ,  $x$ ,  $z$  fixed from a global fit to  $VP\gamma$  and  $V \rightarrow e^+e^-$  decay modes [41, 42, 55];  $e_1$  and  $e_2$  are fixed from a fit [43] to the pion form factor including only  $\pi\pi$  and  $K\bar{K}$  as channels coupling to  $\rho$ .

data independent of the  $\eta/\eta' \rightarrow \pi^+\pi^-\gamma$  decay modes. It is indeed the case for the  $VP\gamma$  or the  $Ve^+e^-$  decay modes and for the pion form factor. As commented on above, these fit values correspond to a very good fit quality for the corresponding data. For instance, they allow to *predict* [32] the two-photon decay widths as recalled in Table 2.

Parameter	PDG 2002	Prediction	Significance ( $n \sigma$ )
$\eta \rightarrow \gamma\gamma$ (keV)	$0.46 \pm 0.04$	$0.46 \pm 0.03$	$0.0 \sigma$
$\eta' \rightarrow \gamma\gamma$ (keV)	$4.29 \pm 0.15$	$4.41 \pm 0.23$	$0.4 \sigma$

Table 2: Partial widths for  $\eta/\eta' \rightarrow \gamma\gamma$  as predicted using Eq. (11) with parameter values as coming from a global (HLS) fit to only  $VP\gamma$  decay modes of light mesons [32].

Choosing the  $\rho$  propagator as it comes out of the HLS fit to the pion form factor [43] is also fairly legitimate, as this  $\rho$  propagator should also be valid anywhere within the HLS framework. As stated above, we consider for clarity only the case where the only open channels are  $\pi\pi$  and  $K\bar{K}$ . We have, nevertheless, checked that changing to various open channel subsets coupling to the  $\rho$  meson (as done in [43] for the pion form factor), with correspondingly changing  $e_1$  and  $e_2$  to their fit values, does not produce any significant modification to the results presented below.

To summarize, self-consistency implies that we can fix all parameters and functions from their most reliable fit values and expressions, provided the data set is independent of the  $\eta/\eta'$  decays considered here. This independent data sample covers  $VP\gamma$  and  $Ve^+e^-$  couplings [41, 42, 32] and the pion form factor [43]. It then follows that all information related with the box anomalies can be *predicted* without any parameter freedom.

## 7 Predictions For $\eta/\eta' \rightarrow \pi^+\pi^-\gamma$ Decays

In this Section, we examine the predictions derived for the  $\eta/\eta' \rightarrow \pi^+\pi^-\gamma$  decay modes for the partial widths and dipion invariant-mass distributions.

### 7.1 Partial Widths, Experimental Values and Predictions

Using Eq. (24) and numerical (and functional) information given in the previous Subsection, it is easy to check that we can write :

$$\Gamma(X \rightarrow \pi^+\pi^-\gamma) = A_X c_X^2 \quad , \quad (27)$$

where :

$$A_X = \frac{1}{36} \frac{\alpha}{[2\pi f_\pi]^6} \int_{2m_\pi}^{m_X} \left| 1 + \frac{3m_\rho^2}{D_\rho(s)} \right|^2 k_\gamma^3 q_\pi^3 d\sqrt{s} \quad , \quad X = \eta, \eta' \quad . \quad (28)$$

This integration can be done by Monte Carlo techniques and gives :

$$A_\eta = 38.25 \pm 1.07 \quad , \quad \text{eV} \quad A_{\eta'} = 42.16 \pm 3.00 \quad \text{keV} \quad . \quad (29)$$

For further concern, one should note that these integrals are not affected by the value for  $x$ . Using the parameter values given in Table 1, Eqs. (19) and (10), one can *compute* the partial widths and get the results collected in Table 3. We have performed the computation by switching on/off the contact term contribution<sup>9</sup>. We stress again that all results presented in this Section do not depend on any free parameter and thus are *predictions* relying on the rest of the HLS phenomenology.

decay	PDG 2002	Prediction with Box Anomaly	Prediction without box Anomaly
$\eta \rightarrow \pi^+\pi^-\gamma$ (eV)	$55 \pm 5$	$56.3 \pm 1.7$	$100.9 \pm 2.8$
Significance ( $n \sigma$ )		$0.25 \sigma$	$8 \sigma$
$\eta' \rightarrow \pi^+\pi^-\gamma$ (keV)	$60 \pm 5$	$48.9 \pm 3.9$	$57.5 \pm 4.0$
Significance ( $n \sigma$ )		$1.75 \sigma$	$0.39 \sigma$

Table 3:  $\eta/\eta'$  Partial widths as predicted by the HLS Model when switching on/off the box anomaly contribution. Significance is computed using an error obtained by adding in quadrature the experimental error and the relevant model error computed by Monte Carlo sampling (using information in Table 1).

<sup>9</sup>When switching off the contact term in Eq. (28), the numbers in Eq. (29) become  $A_\eta = 57.51 \pm 4.01$  eV and  $A_{\eta'} = 49.60 \pm 2.98$  keV, which is already conclusive.

From Table 3, one clearly sees that the *predicted* partial width for  $\eta'$  is not really sensitive to the presence of the contact term. This can be well understood as, indeed, the value for  $A_{\eta'}$  is sharply dominated by the  $\rho$  peak contribution provided by the *VVP* Lagrangian term and the magnitude of the contact term is comparatively small.

In contrast, the *predicted* partial width for  $\eta$  is much more sensitive to the contact term because this contribution has only to compete with the low mass tail of the  $\rho$  distribution ; the bulk of the resonance contribution is indeed sharply suppressed because the available phase space is small and located far outside the  $\rho$  peak.

Therefore, one can already conclude from Table 3 that the  $\eta/\eta'$  partial widths values provide a strong evidence in favor of the box anomaly. Unexpectedly, this evidence is provided by the  $\eta$  partial width alone. Additionally, the values *predicted* for the box anomaly constants  $c_\eta \simeq 1.21$  and  $c_{\eta'} \simeq 1.07$  from the rest of the HLS phenomenology fits nicely the  $\eta/\eta'$  partial widths, which means, for instance, consistency with having  $\theta_P = 10.30^\circ \pm 0.20^\circ$ .

Together with the results predicted for two-photon decay widths of the  $\eta/\eta'$  system, this also gives a strong support to the extended BKY breaking scheme summarized in Section 4 and to Eqs. (11) and (21) for the amplitude expressions at the chiral limit.

## 7.2 Invariant–Mass Spectra With/Without The Contact Term

The shape of the dipion invariant–mass distributions are given in Figure 1, top for  $\eta'$ , mid for  $\eta$ . These are proportional to yields (up to acceptance/efficiency effects). The distributions are displayed with having switched on/off the contact term ; in these two figures, the relative magnitude of the twin distributions is respected.

Looking at the  $\eta$  distributions, one clearly understands the width results given in Table 3, as the integrals corresponding to box anomaly on/off are clearly very different (actually by a factor of about 2).

In the case of the  $\eta$  meson, lineshape differences between the case when the contact term is activated and when it is dropped out are tiny as illustrated by Fig. 1, bottom. In this figure, one displays the distribution obtained by removing the contact term and the one derived by activating it, after rescaling it by  $\simeq 1.8$ .

The lineshape, in the case of the  $\eta'$ , shows that the peak location when accounting for the contact term is slightly higher mass (6 ÷ 8 MeV) compared to the case when this (CT) contribution is cancelled out. However, the main effect is that yields below the  $\rho$  peak location are somewhat suppressed because of the contact term.

In this sort of situation, if one performs a fit of an  $\eta'$  spectrum affected by CT with only a resonance contribution and lets free the resonance parameters, the shape will be distorted. Indeed, in order to average reasonably the rising wing of the  $\rho$  distribution, the peak has to be shifted to higher mass and therefore the observed mass must be larger. This is a mechanical effect connected with the minimization of a  $\chi^2$  for any appropriate function of one variable. We come back to this point when comparing with experimental data.

## 8 Experimental Data on $\eta/\eta' \rightarrow \pi^+\pi^-\gamma$ Decays

There are several sets of data available for the dipion mass spectrum of the  $\eta'$  meson. Most of them have been published only as figures [12, 13, 14, 15, 16, 17]. For these, however, it happens that the information given in the body of the articles provides enough information in order to recover the yields and derive the acceptance/efficiency function ; the redundancy of the information is fortunately such that consistency checks and cross checks can be performed which validate the outcome of the procedure. This is described in details in Section 4 of [33] together with the peculiarities of each of these data sets.

Other spectra were available directly to us [18] or as PhD theses [19, 20, 21, 22] published only as preprints ; Here also the relevant information was either directly available or could be reconstructed accurately, as for the references quoted above. One should note that the data of [21] superseded the ARGUS results published in [14].

These former data samples carry widely spread statistics ; 474 events for the oldest data set [12], 130 events from TASSO [13], 795 events from ARGUS [14] updated three years later to 2626 [21], 321 events in the TPC- $\gamma\gamma$  sample [15], 195 events in the PLUTO data set [19], 586 in the CELLO data set [22], 401 for the data set of WA76 collected using the Omega Prime Spectrometer at the CERN SPS [18] and, finally, 2491 (after acceptance corrections) for the experiment performed at Serpukhov using the Lepton F facility [17].

The method used to extract the dipion invariant-mass spectra from data is of special concern. These were derived from the data samples just listed in the following way : for each bin of dipion invariant-mass, one plots the  $\pi^+\pi^-\gamma$  invariant-mass spectrum and fits with a gaussian (plus a polynomial background) the number of  $\eta'$  it contains. In this way, one get rid to a large extent of the precise background<sup>10</sup> parametrization, as the signal is a narrow gaussian peak dominated by the experimental resolution.

Performing this way, spectra appear without any background and the influence of this in the data sets only reflects in the magnitude of the errors on the yields per bin. It should be stressed that this extraction method is obviously independent of any assumption on the lineshape of the underlying  $\rho$  invariant-mass distribution.

For the data samples of [17, 18, 19], the acceptance/efficiency function was directly known, but without information on its uncertainties. As the spectra of [18, 19] carry small statistics, statistical errors are dominant and errors on the acceptance/efficiency function can be neglected. For the data sample of [17], the acceptance/efficiency function is provided as a curve (see their Fig. 3) ; as no information is reported about uncertainties affecting this function, these cannot be accounted for when folding in this function with any model distribution.

For the other data samples reviewed above, uncertainties on the acceptance/efficiency functions are also unknown, as these can only be derived by unfolding it from the fitting

---

<sup>10</sup>We have to make assumptions on the background shape across some small  $\pi^+\pi^-\gamma$  mass interval while the signal is a narrow gaussian (typically 20 to 30 MeV for its standard deviation). This is certainly much safer than assumptions on the background shape over a 1 GeV invariant-mass interval with on top of this a signal as broad as a  $\rho$  distribution.

distribution. This was always provided as a product of a well defined model function for the decay with this acceptance/efficiency function. This is also of little importance for all data sets dominated by statistical errors, but it also affects the large statistic sample of ARGUS we shall examine [21].

Neglecting this source of uncertainties when computing model errors certainly biases  $\chi^2$  estimates towards larger values (and smaller probabilities). However, it should not spoil qualitatively model descriptions.

The sample of MarkII [16] is also significant ( $\simeq 1200$  events), however, the mass spectrum derived from this has been obtained in a different way : Selecting the events in some mass interval around the  $\eta'$  mass in the *global*  $\pi^+\pi^-\gamma$  invariant-mass spectrum, the corresponding events are plotted in bins of  $\pi^+\pi^-$  invariant-mass. This spectrum is then described as a superposition of a  $\rho$  mass distribution plus some background, and a global fit to this spectrum provides the signal ( $\rho$ ) and background populations inside each bin. Therefore this method assumes an accurate knowledge of all phenomena contributing to the background (and of its parametrization) ; it also relies on the way the  $\rho$  lineshape is parametrized. This is also, basically, the method used to study the  $\eta'$  mass distribution performed by the L3 Collaboration [24] on a sample of  $2123 \pm 53$  events ; this will be specifically discussed at the appropriate place below, as it is the latest published data sample.

Some other papers published spectra without background subtraction (namely [62] and [20] which carry actually the same data). In order to use these, one would have to model the background without any motivated knowledge of the data set and detector properties<sup>11</sup> ; therefore, this MarkII spectrum will not be examined here. This lack of background subtraction is also the reason why the spectrum published by the L3 Collaboration is also skept.

Finally, the most reliable spectrum for the  $\eta'$  decay is the one collected by the Crystal Barrel Collaboration [23] which is also, by far, the largest data sample (7392 events). This spectrum has been constructed using the method described at the beginning of this Section ; therefore, it is independent of any assumption on the underlying  $\rho$  invariant-mass distribution and, thus, is certainly free from any prejudice or bias. Additionally, this data sample is certainly the most secure to be used as uncertainties on acceptance and efficiencies are already included into yield errors and, thus, model comparison can be performed directly and reliably.

The corresponding spectra for the  $\eta$  decay, have been derived from  $\pi p \rightarrow \eta n$  data collected long ago by two experiments [10,11] ; the published data are already background subtracted. They both carry large statistics (7250 for [10] and 18150 for [11]). The relevant results have been published only as figures. Yields per bin can be read off from these figures without any difficulty together with their errors.

In [10], the acceptance/efficiency function is provided directly and also folded in with a well defined model function. It is given superimposed to the case when the analysis

---

<sup>11</sup>Indeed, beside extracting the yields, one needs to estimate the acceptance/efficiency function which might well be different for signal and background events.

is performed with a simple gauge-invariant phase-space matrix element and with a  $\rho$  dominant one. The two corresponding acceptance/efficiency functions are conflicting, essentially in the region  $k_\gamma = 90 \div 110$  MeV. However, this seems to reflect their dependence upon angular distributions. It is therefore worth using the functional information associated with the  $\rho$  dominant matrix element.

For the data of Layter *et al.* [11], the acceptance/efficiency function is not shown and should be unfolded from the theoretical  $\rho$  (and phase-space) distribution(s). This information can be extracted with some reliability ; in contrast with [10], this yields a function extracted from the  $\rho$  distribution very close from those extracted from the simple phase space distribution. Actually, this data set should be considered with some care as extracting the acceptance/efficiency function can only be performed by making some assumption on the  $\rho$  mass actually used in this paper [11]. We have conservatively assumed that Layter *et al.* [11] used the same  $\rho$  mass as Gormley *et al.* [10], namely  $m_\rho = 765$  MeV ; this assumption is crucial and cannot be ascertained. This makes more secure information derived from the Gormley spectrum.

Finally, for both  $\eta$  spectra, it is impossible to restore the accuracy on the acceptance/efficiency function. These will be considered negligible in the present study.

## 9 Experimental Data Versus Predictions For $\eta/\eta'$ Spectra

As seen in Subsection 6.4, the HLS Model provides definite spectra for both  $\eta/\eta'$  invariant-mass distributions. These depend on parameters which can be fixed independently of the  $\eta/\eta' \rightarrow \pi^+\pi^-\gamma$  spectra, like  $a$ ,  $g$ ,  $x$  (see Subsection 6.5), and of the  $\rho$  propagator which is fitted elsewhere [43] with parameters values as determined in these fits (see Eq. (26) and Table 1). The model fairly predicts the absolute magnitude (the integral) of each spectrum as illustrated in Table 3. In this Section, we focus on comparing the *predicted* lineshapes derived from the model Eq.(24) with the data listed in Section 8.

As all data considered are binned, we have integrated the predicted function Eq. (24) (or Eq. (28)) over the bin size and normalized this function to the integral of the experimental distribution. When relevant (*i.e.* all spectra except for the one of Crystal Barrel [23]), the model function was folded in with the acceptance/efficiency function derived for each of the above data samples.

The results are displayed in Figs. (2) to (4). One should note that all  $\eta'$  spectra are given as functions of the dipion invariant-mass, while  $\eta$  spectra are given as functions of the photon momentum in the  $\eta$  rest frame.

In these figures, together with the specific experimental spectrum, we show the predicted curve (computed just as defined just above) when keeping the contact term (full curve) and the one derived by dropping out this contribution (dashed curve). These two cases will be referred to as resp. **CT** and **NCT**. In these figures, we give the  $\chi^2$  corresponding to these two solutions under the form  $\chi^2(\text{CT})/\chi^2(\text{NCT})$ . The number of

degrees of freedom can be easily read off from the spectra as this is exactly the number of bins of the experimental histogram.

The curves shown have been computed at the central values of the parameters as given in Table 1. The  $\chi^2$ 's have been computed by folding in the experimental error in each bin with a model error also computed bin per bin. These model errors have been computed by sampling the parameters around their central values with standard deviations given by their quoted errors (see Table 1). Except for Crystal Barrel [23], where it is irrelevant, uncertainties on the acceptance/efficiency functions are not (cannot be) accounted for. The curves shown are actually histograms which have been smoothed automatically by the HBOOK/PAW package.

Examination of Figs. (2) to (4) is quite interesting. First of all, the spectrum from TPC- $\gamma\gamma$  is clearly the single one far away from predictions, indicating that something was not well controlled when extracting it from data. All others match well, or quite well, the predictions ; this clearly gives support to the model developed in the previous Sections and to the relevance of the parameters given in Table 1.

In terms of probabilities (reflected by the  $\chi^2/dof$  values given in the figures), the oldest data set of [12] gives comparable probabilities to either of the **CT/NCT** assumptions, while maybe slightly preferring the **NCT** assumption. **CT/NCT** descriptions are practically equivalent for the ARGUS [21] and WA76 [18] spectra, while nevertheless slightly favoring the **CT** assumption.

The relatively low statistics spectra provided by TASSO [13] ( $\chi^2$  ratio of 0.6 in favor of the **CT** assumption), CELLO [22] (0.7) and PLUTO [19] (0.7) somewhat prefer the **CT** assumption.

Finally, the two largest statistics experiments Lepton F [17] and Crystal Barrel [23] sharply favor both the **CT** assumption against **NCT** ; the  $\chi^2$  distance is indeed better by more than a factor of 2 .

To be more precise the Lepton F spectrum<sup>12</sup> gives a 3% probability to the **CT** assumption and a  $2 \cdot 10^{-8}$  % probability to the **NCT** assumption. These relatively low probabilities should be related with the lack of information on the acceptance/efficiency function which affects in a same manner both solutions. Accounting for the corresponding errors would certainly increase both probabilities but hardly switch their ordering.

The corresponding probabilities for the Crystal Barrel data set are resp. 57.8% and 0.1 % ; these values are certainly realistic as the model errors are reasonably well accounted for.

Among these two data sets which could be used as reference, the Crystal Barrel data (available in a directly usable form [23]) should clearly be preferred, as systematics are better controlled all along the invariant-mass range. It also carries, by far, the largest statistics.

---

<sup>12</sup>The 8 lowest mass points of this spectrum contribute severely to the  $\chi^2$  for both (**CT/NCT**) assumptions. On the other hand, the sharp drop in acceptance [17] at large  $m_{\pi\pi}$  might have been difficult to estimate reliably. Qualitatively, however, the clear preference of this distribution for the **CT** assumption is obvious.

From  $\chi^2$  values, the shape of the  $\eta$  spectrum from Layter *et al.* [11] seems in better agreement with the **NCT** assumption (77% probability) than with the **CT** assumption (3% probability).

In contrast, the description of the  $\eta$  spectrum from Gormley *et al.* [10] is simply perfect and corresponds to resp. 97.7 % probability for the **CT** assumption and to 58.2 % probability for the **NCT** assumption ; this reflects better the remark following from Fig. 1 (bottom) that these lineshapes are very close together. The  $\chi^2$  values, however, indicate that the geometrical distance ( $\simeq \sqrt{\chi^2}$ ) of this spectrum to the **CT** solution is significantly smaller than those to **NCT**.

Fig. 5 gives the same information as in Fig. (4) but enlarged and binned. Here one sees that a third of the  $\chi^2$  for the Layter spectrum [11] comes from only the bin covering the momentum interval  $60 \div 80$  MeV/c. Compared to the same result for the Gormley spectrum [10], the Layter spectrum looks a little bit skewed. It is, however, impossible to decide whether this comes from systematics affecting the acceptance/efficiency function as this (skewed) shape happens to match nicely the **NCT** assumption<sup>13</sup>.

However, the  $\eta \rightarrow \pi^+\pi^-\gamma$  partial width alone [9], certainly a more secure information, and the Gormley spectrum undoubtedly favor the **CT** assumption against the **NCT** one. These two aspects have to be balanced in a global fit accounting for lineshapes and partial widths.

## 10 A Global Fit to $\eta/\eta'$ Spectra and Widths

We have compared the data (lineshapes and partial widths) with the predictions of our model fed with numerical and functional information coming from the rest of the phenomenology accessible to the HLS framework, without any parameter freedom. The results obtained in Section 7 and 9 considered together indicate that the model is valid and favors the the contact term as a physically motivated contribution to decay processes. We remind that this contact term is *not* a free parameter, as widely discussed above.

In view of this, it looks worth performing a simultaneous fit of the  $\eta$  data sets with some accurate  $\eta'$  spectrum ; for reasons explained above, it is certainly worth choosing the Crystal Barrel spectrum. As a clear conclusion should take into account all aspects of the available experimental information, partial widths have been fed into the  $\chi^2$  to be minimized.

In order to perform this fit one needs to release some of the parameters fixed as in Table 1 ; as the main information for the present purpose is the peak location, it looks worth releasing the parameters named  $e_1$  and  $e_2$  which mostly influence the  $\rho$  peak location. Comparing the values returned from this fit to the corresponding values originally extracted from fitting the pion form factor could contribute to clarify the

---

<sup>13</sup>This skewness might have been magnified unwillingly by the choice of the  $m_\rho$  value we performed in order to extract the acceptance efficiency/function for the Layter spectrum. Any underestimation of this input  $m_\rho$  value contributes to the skewness of this distribution. We are responsible for this uncertainty, but we did not find an unbiased way out.



conclusion, as one can consider the  $\rho$  propagator as a universal function, as valid for  $F_\pi(s)$  as for the  $\eta/\eta'$  spectra.

Indeed, we know that, in the pion form factor, the subtraction polynomials of  $\Pi_{\rho\rho}(s)$  and  $\Pi_{\rho\gamma}(s)$  are somewhat competing and that some (small) correlation among the corresponding polynomials exists [43] ; it is therefore motivated to attempt freeing  $e_1$  and  $e_2$  as these correlations could have spoiled their central values by some (certainly) small amount. However, the parameter values returned from fit must not be inconsistent with their partners derived from fit to the pion form factor only<sup>14</sup>.

On the other hand, the other parameter values in Table 1 describing fairly well the full set of  $V \rightarrow P\gamma$  and  $P \rightarrow V\gamma$  decays would hardly accomodate a significant change of their values without failing to fit the  $VP\gamma$  processes.

In order to avoid too much correlations which can hide clarity in the conclusions, we shall test separately the **CT** and the **NCT** assumptions. Indeed, as the HLS Model predicts the magnitude of the constant contact term (if any), it seems enough to check its precise relevance and no attempt will be made to fit its value. Finally, for the present exercise, we neglect model errors<sup>15</sup> ; this mechanically makes the  $\chi^2$ 's slightly more pessimistic than they really are.

We could have chosen to perform a simultaneous fit of the Crystal Barrel  $\eta'$  data set [23] together with both  $\eta$  data sets [11,10] simultaneously. One could indeed imagine that the systematics could compensate. We have, nevertheless, preferred performing the fits separately for the Crystal Barrel  $\eta'$  spectrum together with each of these  $\eta$  spectra in isolation. Using both  $\eta$  spectra certainly leads to intermediate fit qualities.

Additionally, before letting  $e_1$  and  $e_2$  vary, we have performed the “0 parameter fit” in order to get the  $\chi^2$ 's and probabilities when using directly the parameter values as given in Table 1. In this way, we know the starting quality of the global description of these decay modes induced by the rest of the HLS phenomenology ; we can also estimate what is gained by letting some parameters to vary.

When using the data set of Layter *et al.* [11], while accounting for the  $\eta/\eta'$  contact terms at the expected level (assumption **CT**), one clearly sees from Table 4 that the  $\rho$  lineshape parameters  $e_1$  and  $e_2$  do not move farther than  $2\sigma$  from the values found when fitting the pion form factor [43] (the present  $\sigma$ 's are, however, much larger than found in fits to  $F_\pi(s)$  [43]). The gain in  $\chi^2$  got by releasing these parameters is modest (2.7) and the central values for the partial widths get a little changed. This confirms that the parameter values in Table 1 giving  $\chi^2/dof = 37.88/35$  (34% probability) are already close to optimum ; leaving them free, essentially improves the  $\eta$  spectrum lineshape slightly, but at the expense of slightly degrading the central values of the partial widths.

---

<sup>14</sup>This actually means that a further test could be a simultaneous fit, within a consistent framework, of the pion form factor and of the relevant  $\eta/\eta'$  decay information. One does not expect neither a surprise nor hard difficulties from such an attempt ; the present work indicates that this should not provide more insight than a global probability.

<sup>15</sup>These are certainly present as the uncertainties on  $a$ ,  $g$  and  $x$  contribute to model errors, even when releasing any constraint on  $e_1$  and  $e_2$ .

When dropping out the contact term contributions (assumption **NCT**), the  $\rho$  lineshape parameters  $e_1$  and  $e_2$  change significantly with respect to their starting point, with much larger errors than originally. Even then, the fitted values for  $e_1$  and  $e_2$  move by more than 6 (new)  $\sigma$  from expectations ; therefore, these fitted values can be considered inconsistent with their values fitted in the pion form factor. Additionally, even if the gain is large ( $\chi^2/dof$  is improved from 140.65/35 to 60.88/33), it is not sufficient to push the probability (0.2%) to a reasonable value. Therefore, the peculiar uncertainties affecting this spectrum does not prevent to reach a clear global conclusion.

When using the data set of Gormley *et al.* [10] together with the  $\eta'$  data of Crystal Barrel, the picture is unchanged, but looks much clearer. Fixing the parameters to their values in Table 1, gives already a remarkable fit quality (probability 85 %), when contact terms are accounted for. In this case, letting free  $e_1$  and  $e_2$ , the  $\chi^2$  improves a little (0.57 unit), but the fit probability degrades to 80 %, because of the smaller number of degrees of freedom. The  $\rho$  parameters move by about 1 (new)  $\sigma$  from expectations and thus stay consistent with the  $\rho$  lineshape determined when fitting the pion form factor [43] (the region of the minimum  $\chi^2$  seems flat).

When removing the contact term from our expressions (**NCT** assumption), the starting values of the fit parameters provide a comparatively poor description (1.6 % probability) and the  $\eta$  partial width is far from expectations [9] (see also Table 4). Now, releasing  $e_1$  and  $e_2$  improves significantly the description, as we reach a 27 % probability after fit, with reasonable central values for both partial widths. The price to be paid for this configuration is that the parameters  $e_1$  and  $e_2$  change by more than 3 (new)  $\sigma$  from expectations. Therefore, the **NCT** assumption returns a  $\rho$  lineshape inconsistent with fits to the pion form factor.

From the previous Sections, we already knew that the **CT** assumption is certainly favored in a global account of both shape and partial width for both the  $\eta$  and  $\eta'$  meson simultaneously. We also knew that the **NCT** assumption was disfavored under the same conditions.

What we have learnt in this Section is that, in order to accomodate the description of all aspects of the  $\eta/\eta'$  information, the **NCT** assumption gives up being consistent with the  $\rho$  lineshape as found by fitting the pion form factor [43].

Therefore, we conclude that experimental data do provide a fair evidence in favor of the box anomaly phenomenon at the expected level ; additionally, the sharing observed between resonant and contact term contributions ( $-3 : 1$ ) is well predicted by the FKTUY assumption [30] leading to the Lagrangian in Eq. (5).

In Fig. (6), we show the description of the Crystal Barrel spectrum [23] using Eq. (24) (or Eq. (28)) with the contact term considered and removed. In order to get this we performed fits leaving free  $e_1$  and  $e_2$ .

When accounting for the  $\eta'$  contact term, the  $\rho$  peak location is found in the bin covering the mass region from 725 to 750 MeV. When dropping it out, the (fit) mechanism described in Subsection 7.2 makes the  $\rho$  peak shifting to the next bin which covers the

mass interval from 750 to 775 MeV. This trend was already observed by [17, 23] and also by most Collaborations who have performed extraction of the  $\eta'$  spectrum canonically ; sometime too much [15].

A real shift exists and is small (see Section 7.2). It is artificially increased by the fit procedure in order to get a better account of the low mass tail of the  $\eta'$  invariant–mass spectrum. However, this artificial large mass shift is indeed the signal of the box anomaly.

It is claimed in [24] that the L3 Collaboration does not observe a  $\rho$  peak shift. Several reasons can be invoked. First, as remarked above, [24] did not perform the  $\eta'$  spectrum extraction canonically and, therefore, any conclusion about the underlying  $\rho$  lineshape in the  $\eta'$  decay becomes a delicate matter.

Among other reasons the most likely is their fitting of the  $\rho$  mass and width. The  $\rho$  (Breit–Wigner) mass is thus found at values ( $766 \pm 2$  MeV) normally obtained in only processes where the dynamics is not really well under control (hadroproduction or photoproduction) [9].

If, for a moment, the L3 result were considered as reference in order to detect a  $\rho$  peak shift, one might have instead to consider that a shift occurs in  $e^+e^-$  annihilations or  $\tau$  decays, as these yield rather larger  $\rho$  (Breit–Wigner) masses ( $\simeq 775$  MeV) [9]. Under these conditions, it is difficult to draw any conclusion from [24] about the existence (or absence) of a  $\rho$  peak location shift in the  $\eta' \rightarrow \pi^+\pi^-\gamma$  decay.

## 11 Fits To The Four Anomaly Equations

From now on, we make the assumption that the correct set of equations defining the anomalous amplitudes at the chiral limit are given by Eqs. (11) and (21) and no longer by Eqs. (3). These have been derived using the approximate field transformation Eq.(8). We also examine, for completeness, the case when the exact field transformation is used ; the way to modify our anomaly equations to go from one case to the other is given in the Appendix.

In both cases, these equations actually depend on only one parameter (resp.  $x$  or  $\lambda$ ) ; this can legitimately look like a severe constraint.

### 11.1 Fit Results With Approximate Field Transformation

These equations depend only on  $f_\pi$ ,  $z = [f_K/f_\pi]^2$  and on  $x$ . In the present framework,  $\theta_P$  is no longer an independent parameter as it can be algebraically derived from Eq. (10).

One can consider legitimate to still fix  $f_\pi$  to its experimental value (92.42 MeV) ; this is also true for  $z$  (see Table 1). Therefore, our set of anomaly equations depends on only one parameter  $x$ , we choosed previously to fix from fit results to radiative decays [41, 32]. Releasing the constraint Eq. (10) would only add a comfortable (and useless) parameter freedom to the fits presented just below.

Therefore, one considers here Eqs. (11) and (21) by themselves and attempt to fit them as a constrained system of 4 equations with only *one* unknown ( $x$ ). The results are expected to provide consistency with those obtained for the same parameters and physics quantities derived elsewhere [41, 32] from fit to  $VP\gamma$  decay modes.

The  $\gamma\gamma$  partial widths are related with the amplitudes given in Eqs. (11) by :

$$\Gamma(X \rightarrow \gamma\gamma) = \frac{M_X^3}{64\pi} |G_X(0)|^2 \quad (30)$$

On the other hand, the partial widths  $\Gamma(X \rightarrow \pi^+\pi^-\gamma)$  given by Eq. (27) where the coefficients  $A_X$  given by Eq. (29), depend only on  $\rho$  properties already derived in [43] by a fit to the pion form factor. The errors on  $A_X$  are taken into account in the fit as they are independent of  $x$ .

One has performed a fit of these four partial widths keeping first  $z$  fixed and allowing  $x$  to vary. The results are summarized in Table 5.

It is clear that the fit is fairly successful and represents the most constrained fit of the four partial widths ever proposed. One should remark that the best fit returns a value for  $x$  perfectly consistent with our previous fits to solely the  $VP\gamma$  radiative decays, as can be concluded by comparing to its input value (see Table 1). The corresponding value for  $\theta_P$  is not changed compared to our previous estimates from fit to  $VP\gamma$  decay modes :  $\theta_P = -10.48^\circ \pm 0.18^\circ$ .

We do not give the estimates for derived quantities ( $f_0, f_8, \theta_0, \theta_8$ ) as they practically coincide with the values given in [32] and are all in good correspondence with expectations. Concerning partial widths, three out of four reach a significance much better than the  $1\sigma$  level ; the worst case is  $\Gamma(\eta' \rightarrow \pi^+\pi^-\gamma)$  for which the distance to the recommended value [9] is “only”  $\simeq 1.6\sigma$ .

The fit quality yielded ( $\chi^2/dof = 2.66/3$ ) is such that releasing also  $z$  can look like an academic exercise. It has nevertheless been performed as some correlation could spoil numerically the connection between  $z$  and  $[f_K/f_\pi]^2$ .

The fit returned  $x = 0.908 \pm 0.021$  and  $z = 1.488 \pm 0.054$  with  $\chi^2/dof = 2.62/2$ , practically unchanged, corresponding to a 27 % probability (the worse significance is due to having less degrees of freedom). The correlation coefficient is +0.67, and the minimization does not spoil the numerical values found elsewhere [41, 32] for the same parameters.

Therefore, this leads us to conclude that the  $VP\gamma$  decay modes on the one hand, and the four standard anomalous  $\eta/\eta'$  decay modes on the other hand, yield information fairly consistent with each other. This also means that the anomaly equations we derived are consistent and that the approximate field transformation (leading order in breaking parameters) on which they rely match well the present level of accuracy of the data. This statement will be confirmed directly shortly.

## 11.2 $\theta_P$ versus $x$

Eq. (10) corresponds to setting the EChPT decay constant [2, 3]  $F_\eta^0$  to zero. This is rigorously expressed in the broken HLS model by :

$$\tan \theta_P = \frac{\langle 0 | J_\mu^0 | \eta^8(q) \rangle}{\langle 0 | J_\mu^0 | \eta^0(q) \rangle} = \frac{b_0}{f_0} \quad (31)$$

in term current matrix elements and of their expressions [32]. On the other hand, detailed computation yields :

$$\frac{f_0}{f_\pi} = \frac{2+z}{3x} \quad , \quad \frac{b_0}{f_\pi} = \frac{\sqrt{2}}{3} (1-z) x \quad (32)$$

As clear from its expression  $f_0$  keeps the first non-leading contribution in breaking parameters ( $x = 1 + [x - 1]$ ) ; for  $b_0$  one has naturally chosen to replace  $x$  by 1 and this leads to Eq. (10). However, one may be tempted to keep it and this leads to replace  $x$  by  $x^2$  in the expression Eq. (10) for  $\tan \theta_P$  ; this is nothing but changing the existing term of order  $\mathcal{O}([z - 1][x - 1]) \simeq 0.05$ .

We have redone the fit just described with this change and yielded a slightly better fit quality than the previous one ( $\chi^2/dof = 2.61/3$ ). This fit returns also  $x = 0.902 \pm 0.017$  ( $\simeq 0.5 \sigma$  from its partner in Table 5, or also a one percent change) and no change at all for the partial widths compared to what is displayed in Table 5.

Therefore the sensitivity in describing data is not sharply dependent on non-leading contributions in  $\tan \theta_P$  and using Eq. (10) with  $x$  or  $x^2$  gives undistinguishable results, while the latter might be preferred.

## 11.3 Fit Results With Exact Field Transformation

In order to check the sensitivity of the model to some other details of the broken HLS model, we have also attempted fits using the exact field transformation [32] instead of its leading order approximation (see Eq. (8)) ; some details and formulae are given in the Appendix.

The main motivation was to figure out the sensitivity of the data to the approximation performed on the field transformation.

In this last series of fits, we have kept  $z$  fixed ; therefore the fitting parameters are  $\lambda$  (the basic Nonet Symmetry breaking parameter, see Eq. (7)) and  $\theta_P$ , the later being possibly fixed by the constraint  $\theta_0 = 0$ . The fit results and physics quantities of relevance (ChPT decay constants, mixing angles and partial widths) are given in Table 6.

The first conclusion one can draw from this last Table is that the fit value for  $\theta_0$  departs by less than  $1 \sigma$  from zero and the consequences of this on derived physics quantities is simply negligible. Stated otherwise, the present data are insensitive to releasing the constraint  $\theta_0 = 0$ . This constraint allows to extract a value for  $\theta_8 = -18.2^\circ$  with a very small statistical error ( $\simeq 0.25^\circ$ ) ; The value found for  $f_0$  and  $f_8$  are in the usual ballpark and nothing noticeable appears compared to the case when the approximate field transform was used [32].

The partial widths are still quite consistent with those in Table 5, showing that the refinements introduced by the exact transformation have no impact on the extracted width information for  $\eta/\eta' \rightarrow \gamma\gamma$  and  $\eta/\eta' \rightarrow \pi^+\pi^-\gamma$ .

One might maybe note that, in all our attempts, we never get a solution with the partial width for  $\eta' \rightarrow \pi^+\pi^-\gamma$  larger than its recommended value [9] ; so, the observed 1.6  $\sigma$  departure looks like some small systematic effect. This could be due to having neglected some unidentified tiny (higher order) contribution ; this might also indicate that the recommended value is slightly overestimated.

On the other hand, we have also reconsidered the problem of which value for  $\eta \rightarrow \gamma\gamma$  should be preferred among the the recommended value [9] –recently confirmed by a direct measurement of this branching fraction [65]–, the  $\gamma\gamma$  measurements and the (single) Primakoff effect measurement. This was done already in [32], but with only the  $\eta/\eta \rightarrow \gamma\gamma$  modes. In the present framework extended to the  $\eta/\eta' \rightarrow \pi^+\pi^-\gamma$  decay modes, the conclusion is confirmed : The recommended value is still clearly preferred ; fit quality indicates that it could be slightly smaller (in the direction of the Primakoff measurement), but larger values (in direction of the  $\gamma\gamma$  measurements) are clearly disfavored.

## 12 Summary And Conclusion

The conclusions we get are of various kinds. Therefore, we prefer segmenting into Subsections.

### Experimental Relevance Of The Box Anomaly

Concerning the analysis of a possible occurrence of the box anomaly phenomenon in  $\eta/\eta'$  decays, the main results reported in the present paper can be summarized as follows :

- There is a strong evidence in favor of a contact term contribution in the  $\eta/\eta'$  decays to  $\pi^+\pi^-\gamma$ . All aspects (invariant–mass spectra and partial widths) of the  $\eta/\eta' \rightarrow \pi^+\pi^-\gamma$  decays can be *predicted* with fair accuracy using a few pieces of information coming from fits to  $VP\gamma$  and  $Ve^+e^-$  decay modes in isolation and from information coming from fit to the pion form factor.
- The needed contact term is numerically at the precise value predicted for the box anomaly contribution by the anomalous HLS Lagrangian. This plays a crucial role in yielding, without any fit, the correct dipion invariant–mass spectra and the correct partial widths for both the  $\eta$  and  $\eta'$  mesons.
- If one lets free the parameters defining the  $\rho$  meson lineshape in the  $\eta/\eta'$  spectra, they stay very close to the values expected from (independent) fits to the pion form factor if the predicted contact term is switched on.

In contrast, if one removes this from the amplitudes, the description is poor and can only be improved by letting the  $\rho$  lineshape becoming inconsistent with what is expected from fits to the pion form factor.

- The fit value obtained for the single free parameter ( $x$ , accounting essentially for nonet symmetry breaking) indicates indubitably that a global description of all  $VP\gamma$  modes and of the four  $\eta/\eta'$  decay modes examined here is derived with no additional free parameter.

This leads us to conclude to a strong evidence in favor of the occurrence of the box anomaly phenomenon in  $\eta/\eta' \rightarrow \pi^+\pi^-\gamma$  decays at precisely the level expected from the HLS Model and the WZW Lagrangian.

## Anomaly Equations And Mixing Angles

On the other hand, we have been led to reexamine the validity of the one-angle traditional equations giving the amplitudes for  $\eta/\eta' \rightarrow \gamma\gamma$  and  $\eta/\eta' \rightarrow \pi^+\pi^-\gamma$  at the chiral point, when breaking flavor SU(3) and Nonet Symmetries ; resp. the triangle and box anomaly equations.

We have found that the broken HLS Model leads to one-angle ( $\theta_P$ ) expressions for the anomaly equations which match low energy QCD expectations as expressed by (E)ChPT, but are in deep contradiction with the equations traditionally used.

Instead of depending on three unconstrained parameters, this set of (four) equations we get depends on only one parameter, closely associated with Nonet Symmetry breaking (called  $x$  or  $\lambda$  in the body of the text) ; they also depend on  $z = [f_K/f_\pi]^2$  which can hardly be considered as a free parameter. They are proved to be easily fulfilled by the relevant  $\eta/\eta'$  partial widths with fair accuracy.

Relying on the condition  $\theta_0 = 0$ , well accepted by the existing data, the broken HLS Model leads to an expression of  $\theta_P$  in terms of  $z$  and  $x$  (or  $\lambda$ ) which can be approximated by a simple formula. Additionally, under the same assumption, an equation leading to  $\theta_8 \simeq 2\theta_P$  can be derived.

These equations have been derived from within the framework of the Hidden Local Symmetry Model appropriately broken. The phenomenological success of this mechanism implies that the BKY SU(3) Symmetry breaking scheme, supplemented with Nonet Symmetry breaking can be considered as the relevant breaking mechanism.

This extended BKY breaking scheme forces to a field transformation which admits a reliable approximation valid at leading order in the breaking parameters ( $[z - 1]$ ,  $[x - 1]$ ). The refinements permitted by the exact transformation are found beyond the present accuracy of the experimental data.

## Perspectives

At the level of accuracy permitted by the existing data, the HLS Model (including its anomalous sector) together with the extended BKY symmetry breaking scheme, covers

successfully all aspects of the experimental data examined so far, certainly up to the  $\phi$  mass.

It would be interesting to have improved data in order to check up to which accuracy the HLS framework is predictive. For this purpose, more and better data on the  $\eta/\eta'$  sector would be welcome.

These could come from tau-charm factories (CLEO-C and upgraded BESS) which, running at the  $J/\psi(1S)$ , produce very large samples of  $\eta/\eta'$  mesons under especially clean physics conditions. For instance, in the run at the  $J/\psi(1S)$  foreseen by CLEO-C in 2005  $10^9$  events will be collected. This will provide 860 000  $\eta$  produced opposite in azimuth to a single monoenergetic photon and 2 000 000 opposite to  $\omega/\phi$ . The corresponding  $\eta'$  decay modes will provide samples of about 4 300 000  $\eta'$  produced opposite to a single photon and 500 000 opposite to  $\omega/\phi$ . This should allow an exhaustive study of the  $\eta/\eta'$  system and a much better understanding of low energy QCD.

### Acknowledgements

We gratefully acknowledge V. L. Chernyak (Budker Institute, Novosibirsk) for a critical reading of the manuscript and for valuable remarks and comments. We also acknowledge G. Shore (Swansea University, UK) for useful correspondence and reading the manuscript. Fermilab is operated by URA under DOE contract No. DE-AC02-76CH03000.



# Appendix A

## A1 : The Exact Field Transformation

As stated in Section 4, the field transformation given by Eq. (8) is an approximation of the full transformation which has been derived in [32].

In order to bring the kinetic energy part of the U(3)/SU(3) broken HLS Lagrangian into canonical form (see Eq. (7)), it is appropriate to perform the renormalization in two steps. One first diagonalizes the standard  $\mathcal{L}_{HLS}$  piece using the field transformation Eq. (6). This makes the Lagrangian canonical for the  $\pi/K$  sector, and one yields intermediate fields for the isoscalar sector (double prime fields). In terms of bare fields, we have :

$$\begin{bmatrix} \eta_8'' \\ \eta_0'' \end{bmatrix} = zr \begin{bmatrix} \cos \beta & -\sin \beta \\ -\sin \beta & \cos \beta - \frac{1}{\sqrt{2}} \sin \beta \end{bmatrix} \begin{bmatrix} \eta_8 \\ \eta_0 \end{bmatrix} \quad (\text{A . 1})$$

where, one has defined :

$$r = \frac{\sqrt{(2z+1)^2 + 2(z-1)^2}}{3z} \simeq 0.90 \quad , \quad \tan \beta = \sqrt{2} \frac{z-1}{2z+1} \simeq 0.20 \quad . \quad (\text{A . 2})$$

This transformation brings the kinetic term in the following form [32] :

$$2 \text{ T} = [\partial \eta_8'']^2 + [\partial \eta_0'']^2 + \lambda r [\sin \beta \partial \eta_8'' + \cos \beta \partial \eta_0'']^2. \quad (\text{A . 3})$$

The transformation to fully renormalized fields (primed fields) is performed with :

$$\begin{bmatrix} \eta_8' \\ \eta_0' \end{bmatrix} = \begin{bmatrix} 1 + v \sin^2 \beta & v \sin \beta \cos \beta \\ v \sin \beta \cos \beta & 1 + v \cos^2 \beta \end{bmatrix} \begin{bmatrix} \eta_8'' \\ \eta_0'' \end{bmatrix} \quad (\text{A . 4})$$

where  $v$  carries the real information about Nonet Symmetry breaking (see Eq. (7)) :

$$v = \sqrt{1 + \lambda r^2} - 1 \simeq 0.10 \quad (\text{A . 5})$$

That the transformation combining Eqs. (A . 1) and (A . 4) results, at leading order in the breaking parameters  $[z-1]$  and  $[x-1]$ , into a transformation as simple as Eq. (8), is a little bit unexpected. As noted in the main text, there are several combinations involving  $\lambda$  which are equivalent to  $x$  at leading order ; they are all of the form exhibited by Eq. (9) which is typically a good representation of  $x$  in terms of  $\lambda$ .

This remainder makes clear why  $x$  is influenced by the SU(3) symmetry breaking. A typical expression for  $x$  is :

$$x = \frac{1}{\sqrt{1+v}} \quad (\text{A . 6})$$

## A2 : The Anomalous Amplitudes At The Chiral Limit

The expressions for the anomalous amplitudes at the chiral limit, when using the exact transformation, are easy to get. They amount to the following changes for the triangle anomaly expressions in Eqs. (11) :

$$\begin{aligned} \frac{5z-2}{3z} &\implies \frac{1}{1+v} \left[ \frac{5z-2}{3z} + \frac{v \cos \beta}{rz} \right] && \text{(octet)} \\ \sqrt{2} \frac{5z+1}{3z} x &\implies \frac{1}{1+v} \left[ \sqrt{2} \frac{5z+1}{3z} - \frac{v \sin \beta}{rz} \right] && \text{(singlet)} \end{aligned} \tag{A.7}$$

The octet and singlet combinations for the box anomalies can easily be identified by the occurrence of the  $x$  factor in Eqs. (19) and (21). The changes to be performed there are :

$$\begin{aligned} 1 &\implies \frac{1}{1+v} \left[ 1 + \frac{v \cos \beta}{rz} \right] && \text{(octet)} \\ x &\implies \frac{1}{1+v} \left[ 1 - \frac{v \sin \beta}{rz\sqrt{2}} \right] && \text{(singlet)} \end{aligned} \tag{A.8}$$

It is worth remarking that the exact field transformation changes the  $(\rho\gamma\eta)$  and  $(\rho\gamma\eta')$  coupling constants in such a way that the  $c_X$ 's –modified as just stated– still factor out from their expression. Therefore, Eqs. (18) and (24) keep their structure and the decay invariant–mass spectra for the  $\eta/\eta'$  are the same as for the approximate field transformation.

## A3 : Decay Constants And Mixing Angles

One can express easily the EChPT coupling constants ( $f_0$  and  $f_8$ ) and mixing angles ( $\theta_0$  and  $\theta_8$ ) in terms of the parameters mixing  $\lambda$  and  $\beta$  defined in the previous Subsections.

The following matrix elements of axials currents can be defined in the broken HLS Lagrangian [32] :

$$\begin{aligned} \langle 0 | J_\mu^8 | \pi^8(q) \rangle &= i f_8 q_\mu, & \langle 0 | J_\mu^0 | \eta^0(q) \rangle &= i f_0 q_\mu \\ \langle 0 | J_\mu^8 | \eta_0(q) \rangle &= i b_8 q_\mu, & \langle 0 | J_\mu^0 | \pi^8(q) \rangle &= i b_0 q_\mu \end{aligned} \tag{A.9}$$

One can easily write down the currents and their matrix elements (see [32], Section 6) in the case when the field transformation is not approximated by Eq. (8). Using the notations defined in [32], one finds first :

$$\begin{aligned} \frac{f_8}{f_\pi} &= \frac{rz}{1+v} [1 + v \cos 2\beta] \cos \beta \\ \frac{b_8}{f_\pi} &= -\frac{rz}{1+v} [1 - v \cos 2\beta] \sin \beta \end{aligned} \tag{A.10}$$

Defining the following parameter combinations :

$$h_1 = \cos \beta - \frac{\sin \beta}{\sqrt{2}} \simeq 0.90 \quad , \quad h_2 = \lambda \cos \beta - \frac{1 + \lambda}{\sqrt{2}} \sin \beta \simeq 0.03 \quad (\text{A . 11})$$

one also yields :

$$\begin{aligned} \frac{f_0}{f_\pi} &= \frac{rz}{1+v} \left[ h_1(1+\lambda) + v(2 \cos \beta + h_2) \sin^2 \beta \right] \\ \frac{b_0}{f_\pi} &= -\sin \beta \frac{rz}{1+v} \left[ (1+v \cos 2\beta) - h_1 v \cos \beta \right] \end{aligned} \quad (\text{A . 12})$$

#### A4 : The Condition $\theta_0 = 0$

Phenomenology [32] as well as explicit EChPT computations [58] indicate that the mixing angle  $\theta_0$  is very close to zero. Table 6 clearly illustrates that present data are statistically insensitive to letting  $\theta_0$  departing from zero. Under such conditions, several interesting relations show up.

The definition of the angles  $\theta_0$  and  $\theta_8$  can be expressed in terms of the parameters in Eq. (A . 9) [32]. Using Eq. (A . 12), one can derive :

$$\tan \theta_8 = \tan(\theta_P + \varphi_8) \quad , \quad \tan \theta_0 = -\tan(\theta_P - \varphi_0) \quad (\text{A . 13})$$

where  $\tan \varphi_8 = b_8/f_8$  and  $\tan \varphi_0 = b_0/f_0$  can be explicitly computed. The condition  $\theta_0 = 0$  strictly implies that  $\theta_P = \varphi_0$  which gives :

$$\tan \theta_P = -\frac{1}{1+\lambda} \left[ \frac{\tan \beta}{1 - \frac{1}{\sqrt{2}} \tan \beta} \right] \left[ 1 + \frac{v \tan \beta}{\sqrt{2}} + \dots \right] \quad (\text{A . 14})$$

From Eq. (A . 6), the first term can be interpreted as  $x^2$  and the product of the first two factors is just Eq. (10) for  $\tan \theta_P$  modified with  $x^2$ . With the values for  $v$  and  $\tan \beta$  we have mentioned, the leading correction amounts to only  $1.5 \cdot 10^{-2}$ . If one keeps a  $1/\sqrt{1+\lambda}$  (corresponding to having  $x$  in Eq. (10)) in front of this expression, the correction term gets a additional contribution  $-\lambda/2 \simeq 5 \cdot 10^{-2}$  which becomes dominant. Therefore :

$$\tan \theta_P = \sqrt{2} \frac{(1-z)}{2+z} x^2 \quad (\text{A . 15})$$

could indeed be preferred to Eq. (10).

The second information which follows from  $\theta_0 = 0$  is an approximate relation between  $\theta_8$  and the wave-function mixing angle  $\theta_P$  :

$$\tan \theta_8 = 2 \tan \theta_P \left[ 1 - \frac{\tan \beta}{2\sqrt{2}} + \dots \right] \quad (\text{A . 16})$$

where the leading correction is  $\simeq 7 \cdot 10^{-2}$ .

## References

- [1] J. Gasser and H. Leutwyler, “Chiral Perturbation Theory To One Loop”, *Annals Phys.* **158** (1984) 142. J. Gasser and H. Leutwyler, “Chiral Perturbation Theory: Expansions In The Mass Of The Strange Quark”, *Nucl. Phys. B* **250** (1985) 465.
- [2] H. Leutwyler, “On the  $1/N$ -expansion in chiral perturbation theory”, *Nucl. Phys. Proc. Suppl.* **64** (1998) 223 [arXiv:hep-ph/9709408].
- [3] R. Kaiser and H. Leutwyler, “Pseudoscalar decay constants at large  $N(c)$ ”, arXiv:hep-ph/9806336 ; “Large  $N(c)$  in chiral perturbation theory”, *Eur. Phys. J. C* **17** (2000) 623 [arXiv:hep-ph/0007101].
- [4] J. Wess and B. Zumino, “Consequences Of Anomalous Ward Identities”, *Phys. Lett. B* **37** (1971) 95.
- [5] E. Witten, “Global Aspects Of Current Algebra”, *Nucl. Phys. B* **223** (1983) 422.
- [6] V. V. Solovev and M. V. Terentev, “On  $\text{Eta} \rightarrow \text{Pi Pi Gamma}$ ,  $\text{Eta} \rightarrow 2\text{gamma}$ ,  $\text{Eta} \rightarrow \text{Pi Pi Gamma Gamma}$  Decays And Form-Factor Of The Vector Current In  $K(L4)$  Decay,” *Sov. J. Nucl. Phys.* **16** (1973) 82 [*Yad. Fiz.* **16** (1972) 153].
- [7] Y. M. Antipov *et al.*, “Investigation Of  $\text{Gamma} \rightarrow 3 \text{Pi}$  Chiral Anomaly During Pion Pair Production By Pions In The Nuclear Coulomb Field”, *Phys. Rev. D* **36** (1987) 21.
- [8] B. R. Holstein, “Allowed eta decay modes and chiral symmetry”, *Phys. Scripta* **T99** (2002) 55, [arXiv:hep-ph/0112150].
- [9] K. Hagiwara *et al.* [Particle Data Group Collaboration], “Review Of Particle Physics”, *Phys. Rev. D* **66** (2002) 010001.
- [10] M. Gormley, E. Hyman, W. Y. Lee, T. Nash, J. Peoples, C. Schultz and S. Stein, “Experimental Determination Of The Dalitz-Plot Distribution Of The Decays  $\text{Eta} \rightarrow \text{Pi}^+ \text{Pi}^- \text{Pi}^0$  And  $\text{Eta} \rightarrow \text{Pi}^+ \text{Pi}^- \text{Gamma}$ , And The Branching Ratio  $\text{Eta} \rightarrow \text{Pi}^+ \text{Pi}^- \text{Gamma}/\text{Eta} \rightarrow \text{Pi}^+$ ”, *Phys. Rev. D* **2** (1970) 501.
- [11] J. G. Layter, J. A. Appel, A. Kotlewski, W. Y. Lee, S. Stein and J. J. Thaler, “Study Of Dalitz-Plot Distributions Of The Decays  $\text{Eta} \rightarrow \text{Pi}^+ \text{Pi}^- \text{Pi}^0$  And  $\text{Eta} \rightarrow \text{Pi}^+ \text{Pi}^- \text{Gamma}$ ”, *Phys. Rev. D* **7** (1973) 2565.
- [12] A. Grigorian *et al.* *Nucl. Phys. B* **91** (1975) 232.
- [13] M. Althoff *et al.* [TASSO Collaboration], “Measurement Of The Radiative Width Of The Eta-Prime (958) In Two Photon Interactions”, *Phys. Lett. B* **147** (1984) 487.

- [14] H. Albrecht *et al.* [ARGUS Collaboration], “Measurement Of Eta-Prime  $\rightarrow$  Pi+ Pi-Gamma In Gamma Gamma Collisions”, Phys. Lett. B **199** (1987) 457.
- [15] H. Aihara *et al.* [TPC/Two Gamma Collaboration], “A Study Of Eta-Prime Formation In Photon-Photon Collisions”, Phys. Rev. D **35** (1987) 2650.
- [16] G. Gidal *et al.* [MarkII Collaboration] in “Multiparticle Dynamics 1985”, Proceedings of the XVI<sup>th</sup> International Symposium at Kyriat Anavim (Israel), J. Grunhaus Ed., Editions Frontières, Gif-sur-Yvette, France , 1987.
- [17] S. I. Bityukov *et al.*, “Study Of The Radiative Decay Eta’  $\rightarrow$  Pi+ Pi- Gamma ”, Z. Phys. C **50** (1991) 451.
- [18] T. A. Armstrong *et al.* [WA76 Collaboration], “Study of the pi+ pi- gamma system centrally produced in the reaction p p  $\rightarrow$  p(f) (pi+ pi- gamma) p(s) at 300-GeV/c”, Z. Phys. C **54** (1992) 371.
- [19] M. Feindt, [PLUTO Collaboration], “Research On Two Photon Production Of Eta-Prime Mesons With The Pluto Detector”, DESY-PLUTO-84-03.
- [20] F. Butler [MarkII Collaboration], “Resonant Production In Two Photon Collisions”, LBL preprint FCE 26465, PhD Thesis, Berkeley 1988.
- [21] K. W. McLean [ARGUS Collaboration], Desy Preprint F 15-90-03, PhD Thesis, Hamburg 1990.
- [22] J. H. Peters [CELLO Collaboration], “Production Of Eta, Eta-Prime And F1(1285) Mesons In Tagged And Untagged Two Photon Reactions”, DESY-FCE-90-01.
- [23] A. Abele *et al.* [Crystal Barrel Collaboration], “Measurement Of The Decay Distribution Of Eta-Prime  $\rightarrow$  Pi+ Pi- Gamma And Evidence For The Box Anomaly”, Phys. Lett. B **402** (1997) 195.
- [24] M. Acciarri *et al.* [L3 Collaboration], “Measurement of eta’(958) formation in two-photon collisions at LEP1”, Phys. Lett. B **418** (1998) 399.
- [25] G. Ecker, J. Gasser, H. Leutwyler, A. Pich and E. de Rafael, “Chiral Lagrangians For Massive Spin 1 Fields”, Phys. Lett. B **223** (1989) 425.
- [26] O. Kaymakcalan, S. Rajeev and J. Schechter, “Nonabelian Anomaly And Vector Meson Decays”, Phys. Rev. D **30** (1984) 594 ; O. Kaymakcalan and J. Schechter, “Chiral Lagrangian Of Pseudoscalars And Vectors”, Phys. Rev. D **31** (1985) 1109.
- [27] P. Jain, R. Johnson, U. G. Meissner, N. W. Park and J. Schechter, “Realistic Pseudoscalar Vector Chiral Lagrangian And Its Soliton Excitations”, Phys. Rev. D **37** (1988) 3252.

- [28] U. G. Meissner, “Low-Energy Hadron Physics From Effective Chiral Lagrangians With Vector Mesons”, Phys. Rept. **161** (1988) 213.
- [29] M. Bando, T. Kugo and K. Yamawaki, “Nonlinear Realization And Hidden Local Symmetries”, Phys. Rept. **164** (1988) 217.
- [30] T. Fujiwara, T. Kugo, H. Terao, S. Uehara and K. Yamawaki, “Nonabelian Anomaly And Vector Mesons As Dynamical Gauge Bosons Of Hidden Local Symmetries”, Prog. Theor. Phys. **73** (1985) 926.
- [31] G. Ecker, J. Gasser, H. Leutwyler, A. Pich and E. de Rafael, “Chiral Lagrangians For Massive Spin 1 Fields”, Phys. Lett. B **223** (1989) 425.
- [32] M. Benayoun, L. DelBuono and H. B. O’Connell, “VMD, the WZW Lagrangian and ChPT: The third mixing angle”, Eur. Phys. J. C **17** (2000) 593 [arXiv:hep-ph/9905350].
- [33] M. Benayoun, M. Feindt, M. Girone, A. Kirk, P. Leruste, J. L. Narjoux and K. Safarik, “Experimental evidences for the box anomaly in eta / eta-prime decays and the electric charge of quarks”, Z. Phys. C **58** (1993) 31.
- [34] M. Benayoun, P. Leruste, L. Montanet and J. L. Narjoux, “Meson radiative decays and anomaly physics: A Test of QCD”, Z. Phys. C **65** (1995) 399.
- [35] M. S. Chanowitz, “Radiative Decays Of Eta And Eta-Prime As Probes Of Quark Charges”, Phys. Rev. Lett. **35** (1975) 977 ; “A Test Of Integral And Fractional Charge Quark Models”, Phys. Rev. Lett. **44** (1980) 59.
- [36] F. J. Gilman and R. Kauffman, “The Eta Eta-Prime Mixing Angle”, Phys. Rev. D **36** (1987) 2761 [Erratum-ibid. D **37** (1988) 3348].
- [37] J. F. Donoghue, B. R. Holstein and E. Golowich “Dynamics of the Standard Model”, Cambridge University Press, New York (1992).
- [38] E. P. Venugopal and B. R. Holstein, “Chiral anomaly and eta-eta’ mixing”, Phys. Rev. D **57** (1998) 4397, [arXiv:hep-ph/9710382].
- [39] M. Bando, T. Kugo and K. Yamawaki, “On The Vector Mesons As Dynamical Gauge Bosons Of Hidden Local Symmetries”, Nucl. Phys. **B259** (1985) 493.
- [40] M. Benayoun and H. B. O’Connell, “SU(3) breaking and hidden local symmetry”, Phys. Rev. **D58** (1998) 074006, [arXiv:hep-ph/9804391].
- [41] M. Benayoun, L. DelBuono, S. Eidelman, V. N. Ivanchenko and H. B. O’Connell, “Radiative decays, nonet symmetry and SU(3) breaking”, Phys. Rev. **D59** (1999) 114027, [arXiv:hep-ph/9902326].

- [42] M. Benayoun, L. DelBuono, Ph. Leruste and H. B. O'Connell, "An effective approach to VMD at one loop order and the departures from ideal mixing for vector mesons", *Eur. Phys. J. C* **17** (2000) 303, [arXiv:nucl-th/0004005].
- [43] M. Benayoun, L. DelBuono, P. David, Ph. Leruste, H. B. O'Connell, "The Pion Form Factor Within the Hidden Local Symmetry Model", [arXiv:nucl-th/0301037], to be published in *Eur. Phys. J. C*.
- [44] M. Benayoun, S. Eidelman, K. Maltman, H. B. O'Connell, B. Shwartz and A. G. Williams, "New results in rho0 meson physics", *Eur. Phys. J.* **C2** (1998) 269, [arXiv:hep-ph/9707509].
- [45] S. Rudaz, "Electric Charge Quantization In The Standard Model," *Phys. Rev. D* **41** (1990) 2619.
- [46] A. Abbas, "Anomalies And Charge Quantization In The Standard Model With Arbitrary Number Of Colors," *Phys. Lett. B* **238**, 344 (1990) ; "On the number of colours in quantum chromodynamics," [arXiv:hep-ph/0009242].
- [47] O. Bar and U. J. Wiese, "Can one see the number of colors?," *Nucl. Phys. B* **609**, 225 (2001), [arXiv:hep-ph/0105258].
- [48] O. Hajuj, "Hidden gauge model and radiative decays", *Z. Phys. C* **60** (1993) 357.
- [49] C. Picciotto, "Analysis of eta, K(L)  $\rightarrow$  pi+ pi- gamma using chiral models", *Phys. Rev. D* **45** (1992) 1569.
- [50] T. Feldmann, "Quark structure of pseudoscalar mesons", *Int. J. Mod. Phys. A* **15** (2000) 159, [arXiv:hep-ph/9907491].
- [51] T. Feldmann and P. Kroll, "Mixing of pseudoscalar mesons", *Phys. Scripta* **T99** (2002) 13, [arXiv:hep-ph/0201044].
- [52] M. N. Achasov *et al.*, "Study of the pi pi mass spectra in the process e+ e-  $\rightarrow$  pi+ pi- pi0 at s\*(1/2) approx. 1020-MeV", *Phys. Rev. D* **65** (2002) 032002, [arXiv:hep-ex/0106048].
- [53] A. Aloisio *et al.* [KLOE Collaboration], "Study of the decay Phi  $\rightarrow$  pi+ pi- pi0 with the KLOE detector," *Phys. Lett. B* **561** (2003) 55, [arXiv:hep-ex/0303016].
- [54] R. R. Akhmetshin *et al.* [CMD-2 Collaboration], "First observation of the decay phi  $\rightarrow$  eta-prime(958) gamma", *Phys. Lett. B* **415** (1997) 445.
- [55] M. Benayoun and H. B. O'Connell, "Isospin symmetry breaking within the HLS model: A full ( $\rho$ ,  $\omega$ ,  $\Phi$ ) mixing scheme", *Eur. Phys. J. C* **22** (2001) 503, [arXiv:nucl-th/0107047].
- [56] G. 't Hooft, "How Instantons Solve The U(1) Problem", *Phys. Rept.* **142**, 357 (1986).

- [57] P. J. O'Donnell, "Radiative Decays Of Mesons", *Rev. Mod. Phys.* **53** (1981) 673.
- [58] J. L. Goity, A. M. Bernstein and B. R. Holstein, "The decay  $\pi^0 \rightarrow \gamma\gamma$  to next to leading order in chiral perturbation theory", *Phys. Rev. D* **66** (2002) 076014, [arXiv:hep-ph/0206007].
- [59] C. McNeile and C. Michael [UKQCD Collaboration], "The eta and eta' mesons in QCD", *Phys. Lett. B* **491** (2000) 123, [arXiv:hep-lat/0006020].
- [60] R. R. Akhmetshin *et al.* [CMD-2 Collaboration], "Measurement of  $e^+ e^- \rightarrow \pi^+ \pi^-$  cross section with CMD-2 around rho-meson", *Phys. Lett. B* **527** (2002) 161, [arXiv:hep-ex/0112031].
- [61] J. J. Sanz-Cillero and A. Pich, "Rho meson properties in the chiral theory framework", *Eur. Phys. J. C* **27** (2003) 587, [arXiv:hep-ph/0208199].
- [62] F. Butler *et al.* [MarkII Collaboration], "Measurement Of The Two Photon Width Of The Eta-Prime (958)", *Phys. Rev. D* **42** (1990) 1368.
- [63] H. B. O'Connell, B. C. Pearce, A. W. Thomas and A. G. Williams, "Constraints on the momentum dependence of  $\rho - \omega$  mixing," *Phys. Lett. B* **336**, 1 (1994) [arXiv:hep-ph/9405273].
- [64] B. Mecking *et al.*, "Study of the Axial Anomaly using the  $\gamma\pi^+ \rightarrow \pi^+\pi^0$  Reaction near threshold", CEBAF, Exp. 94-015, Newport News, 1994.
- [65] R. Abegg *et al.*, "Direct Measurement Of The Branching Ratio For The Decay Of The Eta Meson Into Two Photons," *Phys. Rev. D* **53** (1996) 11.



Layter [11]

	$e_1$	$e_2$ (GeV <sup>-2</sup> )	$\chi^2/dof$ (Prob.)	$\eta$ P.W. (eV)	$\eta'$ P.W. (keV)
CT + No Fit	$0.222 \pm 0.011$	$-1.203 \pm 0.017$	37.88/35 (34%)	56.3	48.9
CT + Fit	$0.339^{+0.105}_{-0.056}$	$-1.395^{+0.143}_{-0.160}$	35.16/33 (36.6%)	53.3	46.2
No CT + No Fit	$0.222 \pm 0.011$	$-1.203 \pm 0.017$	140.65/35 (0 %)	100.9	57.5
No CT + Fit	$0.933^{+0.321}_{-0.093}$	$-2.355^{+0.180}_{-0.200}$	60.88/33 (0.2 %)	75.3	40.0

Gormley [10]

	$e_1$	$e_2$ (GeV <sup>-2</sup> )	$\chi^2/dof$ (Prob.)	$\eta$ P.W. (eV)	$\eta'$ P.W. (keV)
CT + No Fit	$0.222 \pm 0.011$	$-1.203 \pm 0.017$	25.58/34 (85%)	56.3	48.9
CT + Fit	$0.269 \pm 0.080$	$-1.275^{+0.135}_{-0.155}$	25.01/32 (80.6 %)	54.6	47.7
No CT + No Fit	$0.222 \pm 0.011$	$-1.203 \pm 0.017$	54.13/34 (1.6%)	76.9	53.4
No CT + Fit	$0.529 \pm 0.090$	$-1.700^{+0.154}_{-0.195}$	36.38/32 (27.2%)	65.7	44.5

Table 4: Simultaneous fits of the  $\eta/\eta'$  distributions from [23, 11] on the one hand, and from [23, 10] on the other hand. CT stand for the “contact terms” generated by the box part of the WZW Lagrangian (see Eq.(5)). The values for  $e_1$  and  $e_2$  quoted in “No Fit” entries are taken from Table 1 and not varied from their central values. The “ P.W.” entries are the central values for the  $\eta$  and  $\eta'$  partial widths in the appropriate units ; the recommended values for these [9] are given in Table 3.

	PDG 2002	Fit Result	Significance (n $\sigma$ )
$x$		$0.911 \pm 0.015$	
$\chi^2/dof$		2.66/3	
Probability		44.6 %	
$\Gamma(\eta \rightarrow \gamma\gamma)$ (keV)	$0.46 \pm 0.04$	$0.46 \pm 0.01$	0.00 $\sigma$
$\Gamma(\eta' \rightarrow \gamma\gamma)$ (keV)	$4.29 \pm 0.15$	$4.34 \pm 0.14$	0.24 $\sigma$
$\Gamma(\eta \rightarrow \pi^+\pi^-\gamma)$ (eV)	$55 \pm 5$	$56.64 \pm 1.71$	0.31 $\sigma$
$\Gamma(\eta' \rightarrow \pi^+\pi^-\gamma)$ (keV)	$60 \pm 5$	$49.75 \pm 3.88$	1.62 $\sigma$

Table 5: Simultaneous fit of the four HLS anomaly equations (Eqs. (11)) and (21) with only  $x$  free (Approximate Field Transformation). First data column gives the recommended values [9].

	PDG 2002	Fit Result $\theta_0$ free	Fit Result $\theta_0 = 0$
$\lambda$		$0.23 \pm 0.06$	$0.21 \pm 0.04$
$\theta_P$		$-10.85^\circ \pm 1.27^\circ$	$-11.48^\circ \pm 0.02^\circ$
$\chi^2/dof$		2.93/2	3.20/3
Probability		23.1 %	36.5%
$\theta_0$		$-1.01^\circ \pm 1.27^\circ$	0
$\theta_8$		$-19.37^\circ \pm 1.29^\circ$	$-18.16^\circ \pm 0.24^\circ$
$f_0$		$1.37 \pm 0.03$	$1.36 \pm 0.03$
$f_8$		$1.34 \pm 0.01$	$1.34 \pm 0.02$
$\Gamma(\eta \rightarrow \gamma\gamma)$ (keV)	$0.46 \pm 0.04$	$0.45 \pm 0.03$	$0.44 \pm 0.01$
$\Gamma(\eta' \rightarrow \gamma\gamma)$ (keV)	$4.29 \pm 0.15$	$4.37 \pm 0.23$	$4.20 \pm 0.17$
$\Gamma(\eta \rightarrow \pi^+\pi^-\gamma)$ (eV)	$55 \pm 5$	$55.38 \pm 2.78$	$55.98 \pm 1.76$
$\Gamma(\eta' \rightarrow \pi^+\pi^-\gamma)$ (keV)	$60 \pm 5$	$49.40 \pm 4.85$	$46.93 \pm 4.00$

Table 6: Simultaneous fit of the four HLS anomaly equations modified by using the exact field transformation. The second data column reports on letting free  $\lambda$  and  $\theta_P$ , while in the third data column only  $\lambda$  is allowed to vary.

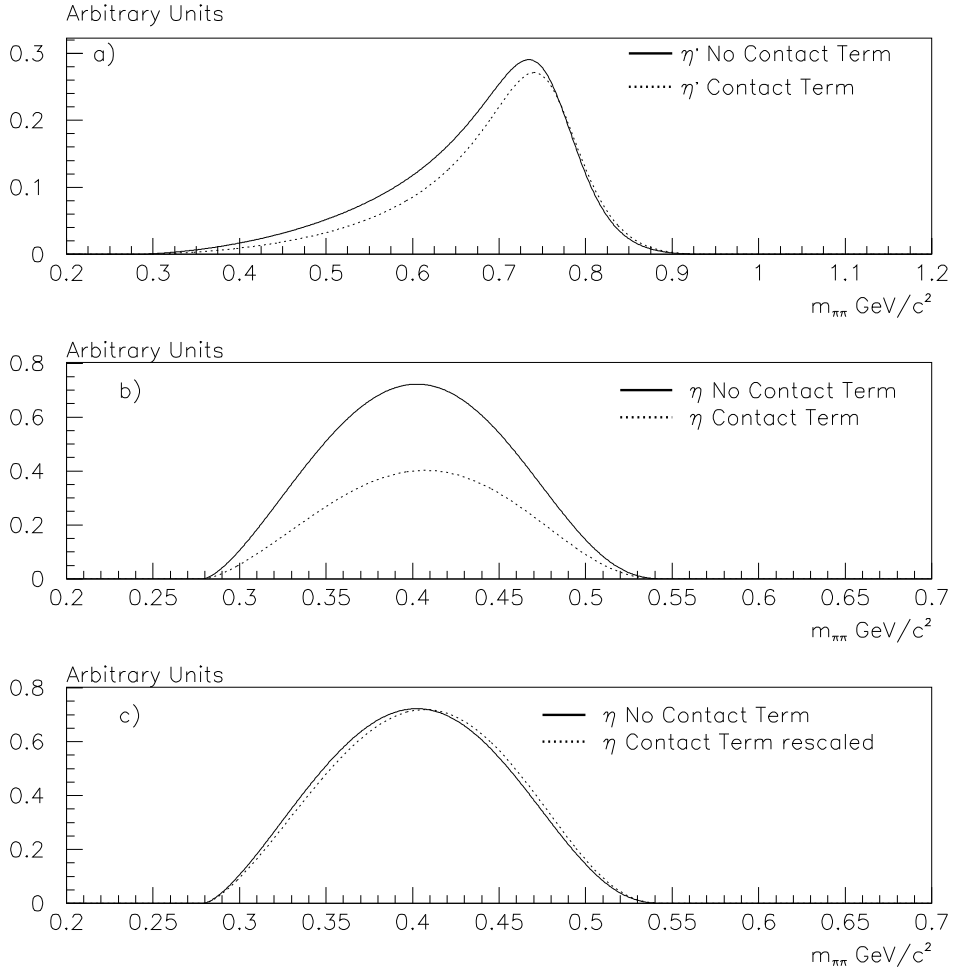


Figure 1:

Predicted shapes for  $\eta'$  (top) and  $\eta$  (mid) distributions as functions of the dipion invariant mass. Full line histograms correspond to having the contact term in the amplitude, dotted line histograms correspond to removing the contact term from the amplitude. All other numerical parameters are at the same values (see Table 1). In the bottom figure, we plot the prediction when accounting for the contact term (rescaled) superimposed with the prediction derived by removing this contribution.

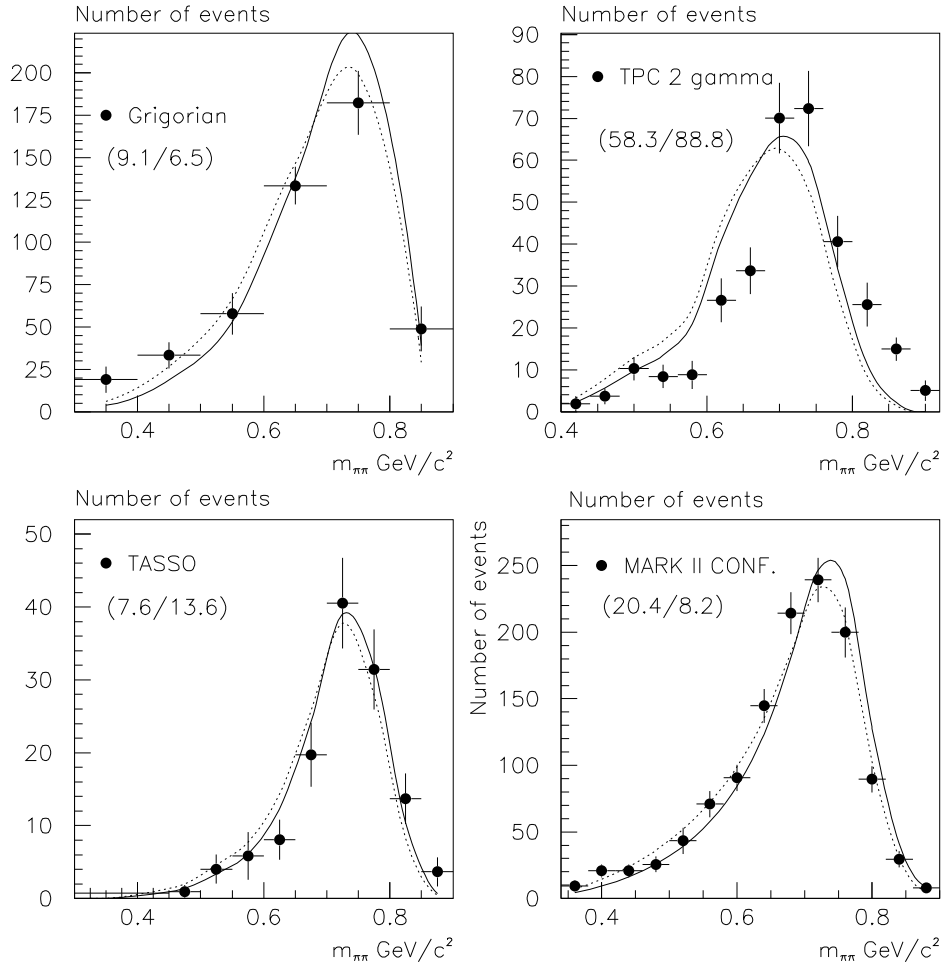


Figure 2:  
 Invariant dipion mass Distributions for  $\eta'$  decay. Experimental data sets with the predicted distributions without the contact term (dashed curve) and with this contribution activated (full curve). The numbers given are  $\chi^2(\text{contact term})/\chi^2(\text{no contact term})$  for the lineshapes only.

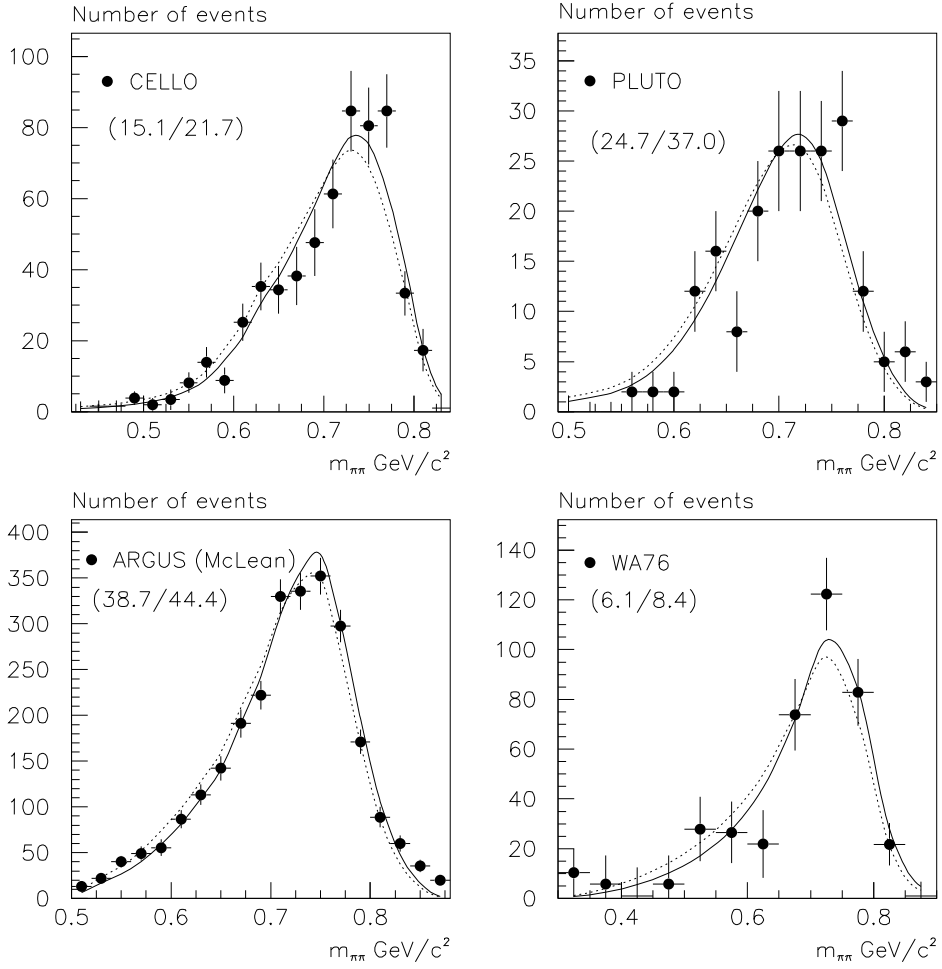


Figure 3:

Invariant dipion mass Distributions for  $\eta'$  decay. Experimental data sets with the predicted distributions without the contact term (dashed curve) and with this contribution activated (full curve). The numbers given are  $\chi^2(\text{contact term})/\chi^2(\text{no contact term})$  for the lineshapes only.

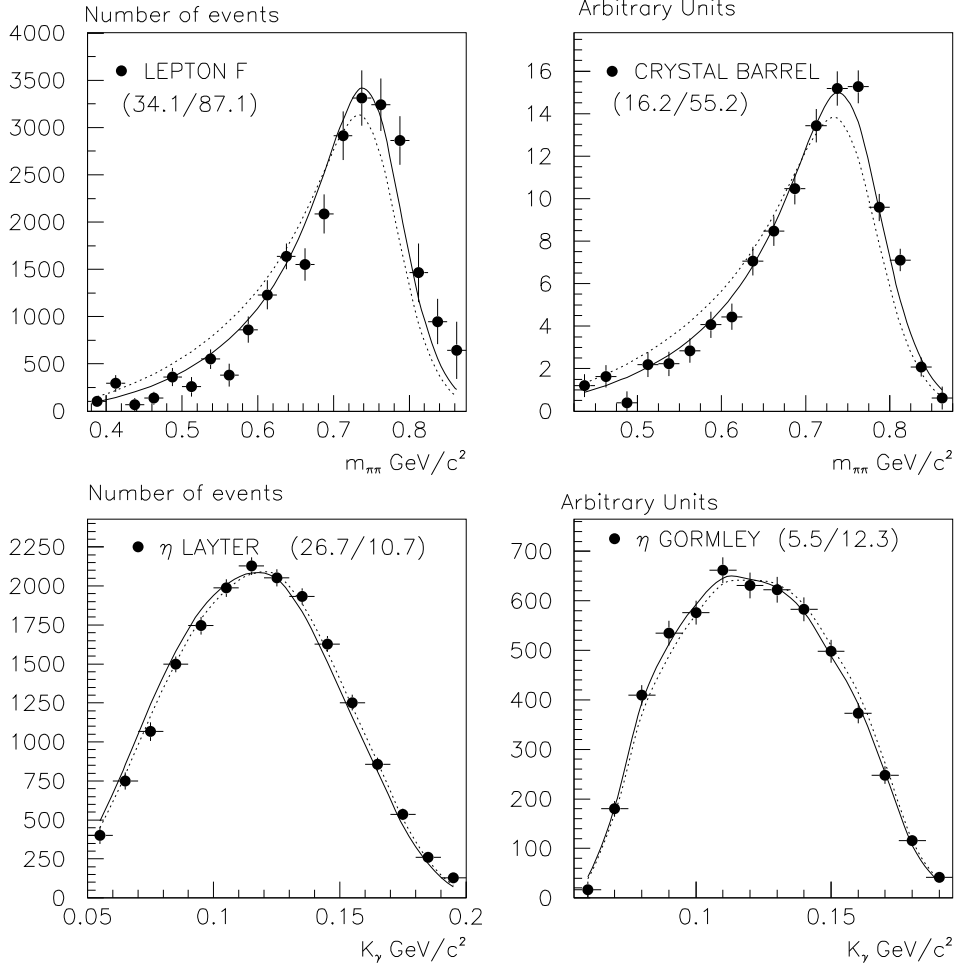


Figure 4:

Invariant dipion mass Distributions for  $\eta'$  decay and the single  $\eta$  decay (as a function of the photon momentum in the  $\eta$  rest frame). Experimental data sets with the predicted distributions without the contact term (dashed curve) and with this contribution activated (full curve). The numbers given are  $\chi^2(\text{contact term})/\chi^2(\text{no contact term})$  for the lineshapes only.

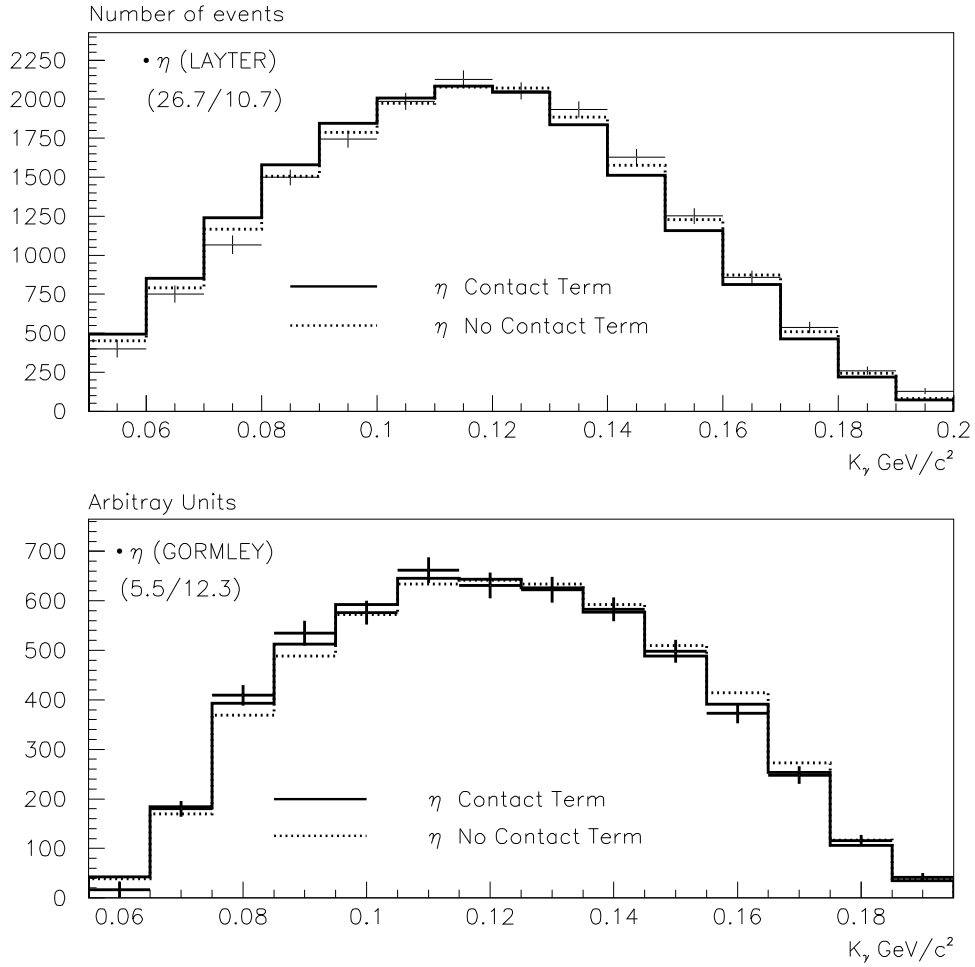


Figure 5:

Photon momentum distribution in  $\eta$  decay. Experimental data are from Layer *et al.* [11] (top), and Gormley *et al.* [10] (bottom); Experimental data sets with the predicted distributions without the contact term (dashed curve) and with this contribution activated (full curve). The numbers given are  $\chi^2(\text{contact term})/\chi^2(\text{no contact term})$  for the lineshapes only.

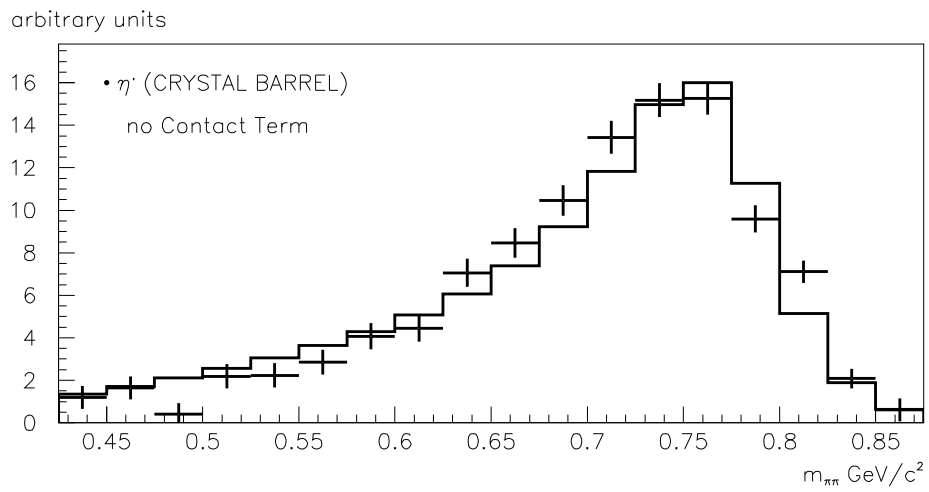
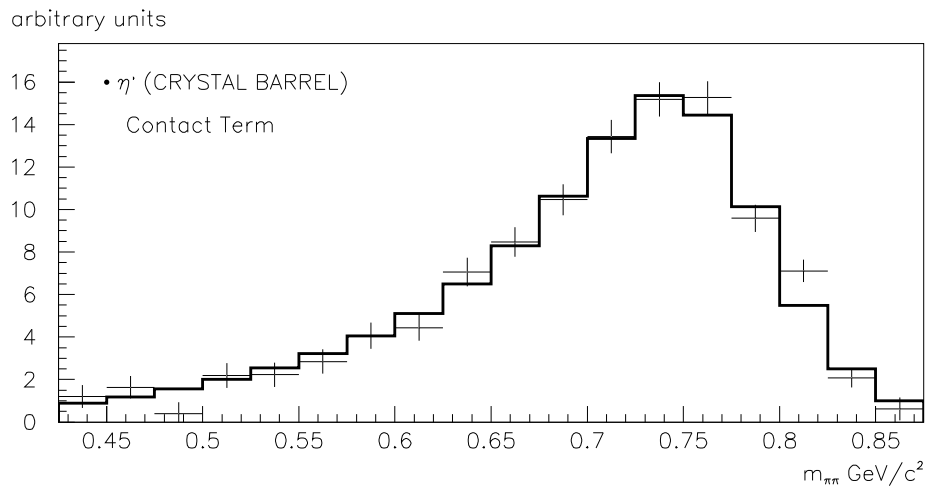


Figure 6:  
Fit of the  $\eta'$  invariant mass spectrum, top by including the contact term, bottom by removing this term. Compare the peak locations.